

[Interactive
Comment](#)

Interactive comment on “Fluctuations of a Greenlandic tidewater glacier driven by changes in atmospheric forcing: observations and modelling of Kangiata Nunaata Sermia, 1859–present” by J. M. Lea et al.

M. Pelto

mauri.pelto@nichols.edu

Received and published: 4 May 2014

Lea et al (2014) provide a detailed presentation of the results of a simple flow-band numerical model for reconstructing glacier dynamics and the terminus behavior of Kangiata Sermia. They further compare the resulting terminus history to sea surface temperature and air temperature finding this glacier more sensitive to the latter. This model provides useful insights and the results here will be of considerable importance, in part because the glacier has a sill preventing sea water at depth from entering the fjord. The paper needs more attention to the fjord width variable to better quantify the importance

[Full Screen / Esc](#)

[Printer-friendly Version](#)

[Interactive Discussion](#)

[Discussion Paper](#)



and limitations of this parameters impact on terminus behavior.

Specific Comments:

09-25: List a couple of example glaciers, where warm water incursion is important.

2010-3: Other glaciers with shallow sills in their fjords? Should have a better Figure 1 that illustrates the larger region and points out the sill location and other key features, this is a long and complicated fjord. This could replace Figure 3. The figure could be similar to Figure 1 from Lea and others (2014a) but showing the sill location too. Any bathymetry that can be added could be in this figure also.

11-25: Example here from Lea et al (2014b) in the difference maybe Jakobshavn or Narssap Sermia.

13-14: Explain crucial nature of the crevasse water depth variable.

14-5: The model is not focused on the seasonal cycles as noted, but as a follow up to the runoff cycle, the velocity cycle should be mentioned in the next sentence. Ahlstrøm et al (2013) in their Figure 4 indicate the peak in velocity as the melt season begins and a decline and minimum in velocity as the melt season progresses.

16-10: What is the upstream limit where rapid ice flow begins, identified by Joughin et al (2010) and modeled by Lea et al (2014a)? Does this agree with the velocity and depth profile in Thomas (2009)?

19-26: Fjord width and pinning point importance. Given the nature of the model and lack of bathymetry it is not expected that this be fully quantified here, since pinning points can be width or depth based. Fjord orientation may also be involved, less so for Kangiata. However, it should be emphasized more. In Figure 1 and 3 it would appear that natural pinning points exist at the LIA maximum, the 1921-1936 terminus location and the 1979-1997 terminus position. It makes sense to have an along track fjord width figure, which would show how much control this factor play in short term slowing or accelerating the retreat. This could be one slice of Figure 4a, which would

Full Screen / Esc

Printer-friendly Version


Interactive Discussion

Discussion Paper




show fjord width as a function of time not distance. Carr et al (2013 and 2014) provide a good description of the concept first outlined by John Mercer (1961). From Carr et al (2014).

"However, our data suggest that along-flow variations in fjord width are an important control, and we demonstrate a statistical relationship between fjord width variability and glacier retreat across the study region. We suggest that along-flow width variations may influence retreat rates via two mechanisms: (1) owing to the principle of mass conservation, widening of the fjord would mean that the glacier needs to thin and the surface slope needs to reduce in order to maintain the same ice flux, which would make the ice more vulnerable to thinning and eventually to flotation, thus increasing calving rates and promoting retreat; and (2) lateral resistive stresses tend to decrease with increasing width, which would reduce resistance to flow and promote further dynamics thinning and retreat."

 21-25: Need to provide an example Mbase value that the reader can better relate to, mean thickness of melt. What is the areal extent where submarine melting occurs, what is its variability in the model?

2023-8: This is the natural location to discuss fjord width role in changing retreat rates, if the model indicates it is a key factor at such points. If not that is key to point out to.

 25-7: Specify the centennial behavior referred to here.

 25-21: The fjord width as noted cannot be verified above the 2012 position, however, it can be stated whether your work suggests it increases and how far behind the current terminus there is a significant change. Is there an inflection in surface slope at some distance above the terminus suggesting a depth pinning point?

Ahlström, A. P., et al: Seasonal velocities of eight major marine-terminating outlet glaciers of the Greenland ice sheet from continuous in situ GPS instruments, Earth Syst. Sci. Data, 5, 277-287, doi:10.5194/essd-5-277-2013, 2013.

[Full Screen / Esc](#)[Printer-friendly Version](#)[Interactive Discussion](#)[Discussion Paper](#)

Carr, J.R., Stokes, C.R. and Vieli, A., in press. Recent retreat of major outlet glaciers on Novaya Zemlya, Russian Arctic, influenced by fjord geometry and sea-ice conditions. *J. Glaciology*, 60, doi: 10.3189/2014JoG13J122, 2014.

Carr, J.R., Vieli, A. and Stokes, C.R.: Climatic, oceanic and topographic controls on marine-terminating outlet glacier behavior in north-west Greenland at seasonal to interannual timescales. *Journal of Geophysical Research*, 118(3), 1210-1226, 2013.

Joughin, I., Smith, B. E., Howat, I. M., Scambos, T., and Moon, T.: Greenland flow variability from ice-sheet-wide velocity mapping, *J. Glaciol.*, 56, 415–430, doi:10.3189/002214310792447734, 2010.

Mercer, J.H.: The Response of Fjord Glaciers to changes in the Firn Limit. *J. Glaciology*, 3(29), 850-858, 1961.

Thomas, R, Frederick, E, Krabill, W, Manizade, S, and Martin, C.: Recent changes on Greenland outlet glaciers. *J Glaciology*, 55(189), 147-162, 2009.

[Interactive comment on The Cryosphere Discuss.](#), 8, 2005, 2014.

[Full Screen / Esc](#)[Printer-friendly Version](#)[Interactive Discussion](#)[Discussion Paper](#)

[Interactive
Comment](#)

Interactive comment on “Fluctuations of a Greenlandic tidewater glacier driven by changes in atmospheric forcing: observations and modelling of Kangiata Nunaata Sermia, 1859–present” by J. M. Lea et al.

Anonymous Referee #1

Received and published: 5 June 2014

This paper is a solid and original contribution that tests the ability of a model to replicate observed terminus position over ca. 150 years and investigates the possible controls upon the terminus position. In this respect, it adds to our understanding of the performance of models over important timescales whilst at the same time providing insight into the controls on terminus position in the KNS region. Overall, I found this a useful and interesting manuscript which is well-written and has good quality figures. As outlined below, there are a few points which could help clarify the paper, the most significant of which is providing a little more information on the shape control exerted (or

[Full Screen / Esc](#)

[Printer-friendly Version](#)

[Interactive Discussion](#)

[Discussion Paper](#)



not exerted) by the fjord sides and bed.

☰ would benefit from seeing a more clearly defined set of aims and objectives at the end of section 1. The objectives are effectively there (present record, evaluate model, test sensitivities), but crystallising the aim would aid clarity.

☰ line 10 on page 2010, is there any quantified uncertainty associated with the HadISST data? If so, do you incorporate any uncertainty range in your SST time series?

☰ the start of section 3, it might be good to start with the indication of the kinds of data you will map from. Then go on to describe the LIA max and later terminus positions.

☰ around lines 10-20 on page 2011, were there any cases where multiple images were available for a single year, and if so, does that help you indicate the confidence with which you can say the terminus position from a particular year is robust and not subject to high variability within the summer months?

In the model description at the start of section 4: You could indicate that the model uses

☰ stretched grid, enabling small adjustments in resolution which is one of the keys to robust grounding line tracking. Note that in table 2, you indicate grid size is ~250 m, but of course this will shrink a little, so include the explanation in the text, and in the table you could call it ☰ initial grid size. Also, how do you prescribe ☰ basal slip conditions?

☰ though you have no seasonal sliding variability, does basal slip evolve in response to changing ice conditions (e.g. as a function of driving stress?).

☰ section 4.1, you introduce a new parameterization dwnew. Perhaps indicate, in a single sentence, why it is unrealistic to follow the Nick approach of having such a restriction. The answer is obvious, but it would help show your thinking.

☰ line 15 of page 2022, you state talk about topographically controlled retreat. Can you be more specific about what you mean by this? E.g. retreat from a lateral or a vertical pinning point? I think that in sections 7.1 and 7.2 you need to be clearer about the

Full Screen / Esc


Printer-friendly Version


Interactive Discussion


Discussion Paper





influence of topography on both the observed and the modeled retreat rates. It would be good to see a plot of fjord width and fjord depth next to your modeled terminus position graphs (Fig. 5). You could also plot what lateral and basal drag looks like when the model is at its LIA position as it would show where peaks in drag may occur and may exert relatively more or relatively less influence.

 **line 19-20 on page 2024**, I am not clear how ocean forcing (via SST) could dominate atmospheric forcing (via surface runoff). I.e. although the forward case makes sense, in the vice versa case, why would SST alter surface runoff? Perhaps I do not understand the sentence?

 **line 17 on page 2025**: You don't appear to state anywhere in the earlier parts of the paper how you define fjord width for the model input. You should state this somewhere.

 **could be useful** to have a figure showing the DEM (above and below sea level) so that we can see what the fjord bed looks like in conjunction with the fjord margins on land. This may aid the communication about the topographic control vs. the climate vs. ocean control.

 **figure 1**: I found it hard to tell which colored line is from which year in panel B. I would prefer to see a more specific legend rather than a graduated color scale.

 **figure 5A**, it would be useful to have dots at each point on the black line to indicate where you have a real data point.

Interactive comment on The Cryosphere Discuss., 8, 2005, 2014.

[Full Screen / Esc](#)[Printer-friendly Version](#)[Interactive Discussion](#)[Discussion Paper](#)

[Interactive
Comment](#)

Interactive comment on “Fluctuations of a Greenlandic tidewater glacier driven by changes in atmospheric forcing: observations and modelling of Kangiata Nunaata Sermia, 1859–present” by J. M. Lea et al.

S. Price (Referee)

sprice@lanl.gov

Received and published: 20 June 2014

Summary

In this paper a novel model validation exercise, with relevance to Greenland ice sheet outlet glaciers, is presented and discussed. The authors begin by motivating efforts for the validation of outlet glacier models on century to decadal timescales and by summarizing past studies that support an oceanic and atmospheric influence on controlling outlet glacier terminus position over time. They suggest that locations for which

[Full Screen / Esc](#)

[Printer-friendly Version](#)

[Interactive Discussion](#)

[Discussion Paper](#)



decadal to century-scale records of both climate (in this case, air and sea surface temperatures) and outlet glacier terminus position exist should provide good test cases for both validating numerical models and for better understanding relationships between outlet glacier terminus change and climate forcing. Kangiata Nunaata Sermia (KNS) glacier in SW Greenland, during the period 1859 to the present, is identified as one such location. A summary of the available climate and outlet glacier terminus position data is then provided, as is a description of the flowband model used and the methods for linking available climate records to dynamic changes within the model. A Monte Carlo approach for generating forward model runs (as a function of unknown model parameters) is presented, as is the procedure for identifying acceptable runs for further examination. From the discussion and conclusions sections that follow, the important findings from the work:

- 1) Periods of terminus retreat that are NOT topographically controlled generally coincide with periods of positive air and sea-surface temperature anomalies, provided that the air and sea-surface temperature records are averaged over suitably long time periods. It is suggested that records of climate and/or terminus position on the order of 2-5 years in duration will be too short (too noisy) to be relevant.
- 2) Care must be taken when looking for correlations between climate and outlet glacier terminus retreat because topographically controlled phases of retreat may or may not be in phase with air and sea-surface temperature anomalies.
- 3) When comparing observed terminus positions to model results, multi-annual time averages of positions should be used, in order to remove inherent noisiness due to the stochastic nature of calving.
- 4) For model runs in which terminus retreat is representative of observations, some combination of both oceanic and atmospheric forcing are necessary to induce the modeled terminus positions. While atmospheric forcing appears to be the more important of the two for KNS, some secondary link between atmospheric forcing and ocean forcing

[Full Screen / Esc](#)[Printer-friendly Version](#)[Interactive Discussion](#)[Discussion Paper](#)

cannot be ruled out (e.g., changes in melting and runoff affecting fjord circulation).

Overall, this paper was well organized, well written, and easy to read. The science questions addressed are well within the scope of TC. The authors reach interesting and substantial conclusions, both with respect to demonstrating that their model can reasonably reproduce an observed outlet glacier retreat history and with respect to improving our understanding of (i) the relative importance of atmospheric vs. oceanic forcing in causing the observed retreat and (ii) the relevant time periods over which models and observations of outlet glacier terminus behavior should be compared over. The various datasets (the outlet glacier terminus position time series, the climate data time series) and new developments (metrics and weight for model evaluation) put into the study are a nice addition to the currently very small number of real-world, model validation exercises. They may prove useful to other modeling groups in the future (e.g., if some additional work were done to set this study up as a standard “validation” test case).

The paper doesn't require any major revisions, but I have a few minor suggestions (below) that might make the paper more clear and readable.

Minor Concerns

[Section or page number, line number(s): comment]

≡ **abstract, 15-16:** "... with changes in atmospheric forcing not needing to be offset by changes in oceanic forcing sensitivity." After reading the full paper, it is more clear what is meant by this statement, but as written it is not clear what is meant by this in the abstract.

≡ **10, 8:** "...used to good effect...". This is kind of vague. Can you clarify further if/how the papers referenced support the argument that SSTs are a good reference for oceanic forcing?

≡ **10, 10-17:** Clarify if/that the data you are referring to are reanalysis data.

[Full Screen / Esc](#)[Printer-friendly Version](#)[Interactive Discussion](#)[Discussion Paper](#)

12, 17: A steady-in-time SMB relationship is used. It would be good to discuss whether or not the model output is sensitive to this, or at least present arguments for why it is not (especially since, from other sections, it sounds like there are time varying SMB fields that could be used to allow for an SMB that varies in time).

13, 3-4: While it is certainly not necessary to repeat the entire init. cond. tuning procedure here, it would be nice if a short summary was given (so that the reader does not have to refer to Lea et al. (2014a) if they don't want to).

13-2014: It would be nice to know how the value of R_{base} is determined. It sounds like it probably comes from the models mentioned in the next section, "definition of B_{month} ", but that is not entirely clear.

15: suggest elaborating on the title of the section "confluence with AS", to make it clear up front that you will also talk about how the ice flux is affected by this (e.g., "Confluence with AS: adjustments to d_w and ice flux").

17, 12-19: From the description given, it is not entirely clear how the model parameters, which are varied according to the Monte Carlo procedure, are treated during the model initialization.

18, 1-2: In general, the use of the "=" when describing a variable seems awkward (e.g. " n =terminus observation"). Perhaps it is just a stylistic preference, but it seems like it would be clearer to use something like " n represents a particular terminus observation, k represents the total number of terminus observations," etc.

18-2019: The section on the reconstruction of glacier terminus positions seems a bit oddly placed. Might it go better earlier on in the paper, before the model is discussed? Or, perhaps maybe even in a short appendix?

23, 5-8: Put another way, the sign of advance or retreat taken from observations is likely to be a more robust indicator than the inferred rate of advance or retreat (?).

Conclusions: You might add something about whether or not this work could be ex-

panded into a standard test case for use in validating models that aim to simulate outlet glacier retreat and/or models that aim to simulate calving and its impact on outlet glacier dynamics.

Tables

Table 2: It would be nice to know the approx. temperature that the choice of the Glenn's law constant $A(T)$ corresponds to (and how it was chosen).

Figures

Figure 3: In my printed version of this figure, the photograph is very dark and hard to see. It is not quite as bad in the digital version, but still not great. Perhaps the authors could play with the contrast / brightness of this image a bit to improve it?

Figure 5: It might be instructive to include a few “failed” runs on this plot for reference. And / or perhaps a run where retreat occurs but forcing is simply held constant in time. This would give the reader a general sense for how sensitive the model is to the time-dependent aspect of the climate forcing.

Editorial

A .pdf file, with some minor editorial suggestions, is attached. Note that one probably needs to use an Adobe product to see all of these (e.g. Mac Preview will show some, but not all of the suggested edits).

Please also note the supplement to this comment:

<http://www.the-cryosphere-discuss.net/8/C955/2014/tcd-8-C955-2014-supplement.pdf>

Interactive comment on The Cryosphere Discuss., 8, 2005, 2014.

Interactive
Comment

Full Screen / Esc

Printer-friendly Version

Interactive Discussion

Discussion Paper



This discussion paper is/has been under review for the journal The Cryosphere (TC).
Please refer to the corresponding final paper in TC if available.

Fluctuations of a Greenlandic tidewater glacier driven by changes in atmospheric forcing: observations and modelling of Kangiata Nunaata Sermia, 1859–present

J. M. Lea¹, D. W. F. Mair¹, F. M. Nick^{2,3}, B. R. Rea¹, D. van As⁴, M. Morlighem⁵,
P. W. Nienow⁶, and A. Weidick⁴

¹Department of Geography and the Environment, University of Aberdeen, Elphinstone Road, AB24 3UF, UK

²The University Centre in Svalbard (UNIS), P.O. Box 156, 9171 Longyearbyen, Norway

³Centre for Ice and Climate, Niels Bohr Institute, University of Copenhagen, Copenhagen, 2100, Denmark

⁴Geological Survey of Denmark and Greenland (GEUS), Copenhagen, Denmark

⁵University of California, Irvine, Department of Earth System Science, Croul Hall, Irvine, CA 92697-3100, USA

⁶School of GeoSciences, University of Edinburgh, Drummond Street, Edinburgh, EH8 9XP, UK

2005

Received: 4 April 2014 – Accepted: 14 April 2014 – Published: 24 April 2014

Correspondence to: J. M. Lea (j.lea@abdn.ac.uk)

Published by Copernicus Publications on behalf of the European Geosciences Union.

2006

Abstract

Many tidewater glaciers in Greenland are known to have undergone significant retreat during the last century following their Little Ice Age maxima. Where it is possible to reconstruct glacier change over this period, they provide excellent records for comparison to climate records, and calibration/validation for numerical models. These records therefore allow tests of numerical models that seek to simulate tidewater glacier behaviour over multi-decadal to centennial timescales. Here we present a detailed record of behaviour from Kangiata Nunaata Sermia (KNS), SW Greenland, between 1859–2012 and compare it against available oceanographic and atmospheric temperature variability between 1871–2012. We also use these records to evaluate the ability of a well-established one-dimensional flow-band model to replicate behaviour for the observation period. The record of terminus change demonstrates that KNS has advanced/retreated in phase with atmosphere and ocean climate anomalies averaged over multi-annual to decadal timescales. Results from an ensemble of model runs demonstrate that observed dynamics can be replicated, with changes in atmospheric forcing not needing to be offset by changes in oceanic forcing sensitivity. Furthermore, ~~successful~~ runs ~~always~~ require a significant atmospheric forcing component, ~~while an~~ oceanic forcing component is not always needed. Although the importance of oceanic forcing cannot be discounted, these results demonstrate that changes in atmospheric forcing are likely to be a primary driver of the terminus fluctuations of KNS from 1859–2012.

1 Introduction

Calving from tidewater glaciers (TWGs) accounts for up to 50 % of the mass loss from the Greenland Ice Sheet (Van den Broek et al., 2009). Thus determining controls on tidewater glacier dynamics over decadal to centennial timescales is crucial to understanding their contribution to sea level in a warming climate (Alley et al., 2010; Vieli

2007

and Nick, 2011). ~~The ability to achieve this in~~ Greenland has been restricted in part by the relative lack of TWG terminus observations prior to the satellite age, and evidence of terminus locations ~~being spread across a disparate array of sources~~. However, the synthesis of these ~~sources~~ has previously allowed multi-decadal to centennial records of TWG glacier behaviour to be reconstructed (e.g. Csatho et al., 2008; Björk et al., 2012; Weidick et al., 2012).

~~The generation of such records~~ provide potentially excellent calibration and validation records for numerical modelling efforts (Vieli and Nick, 2011). That is to say that numerical models that are capable of replicating observed terminus behaviour over decadal to centennial timescales will be better placed to predict the future behaviour of a TWG over similar timescales. Despite this, there remain few examples of modelling efforts that have attempted to calibrate their results against multi-decadal observational records (e.g. Colgan et al., 2012). The ability of most numerical models to replicate dynamics over such timescales using realistic inputs therefore remains largely untested.

By undertaking calibration/validation exercises, the sensitivity of terminus position to different climatically forced processes can also be evaluated (e.g. Nick et al., 2013; Cook et al., 2013; Lea et al., 2014a). This is achieved by comparing the sensitivity of a modelled glacier to climate forcing against **observed behaviour** (Nick et al., 2013). With a knowledge of realistic ranges of forcing, this allows evaluation of the relative importance of each in contributing to the observed TWG behaviour.

Changes in oceanic forcing are significant drivers of TWG retreat in Greenland (Murray et al., 2010; Straneo et al., 2010; Rignot et al., 2012), but their relative importance between glaciers appears to be dependent on geographical location, glacier geometry (Nick et al., 2013), and potentially fjord connectivity with the open ocean (Straneo et al., 2012). Model based studies have also helped to demonstrate the sensitivity of some major outlet glaciers to air temperature changes (via enhanced runoff increasing crevasse water depth; Nick et al., 2013; Cook et al., 2013).

Where multi-decadal to centennial timescale climate data exist alongside records of terminus position, these provide the potential for robust evaluation of both numer-

2008

Where the full terminus cannot be observed in photographs, terminus position is determined indirectly using GIS based analyses described below, in conjunction with evidence from maps (e.g. [Lea et al., 2014a](#)). Subsequent to 1921, intermittent direct observations of the terminus are available enabling mapping of terminus positions from a combination of ground-based, oblique-aerial, vertical-aerial, and satellite imagery (list of sources in Table 1).

Landsat panchromatic band imagery was used to map terminus position for 1987–2012. Cloud-free Landsat scenes were selected for analysis, acquired as close to the melt season as possible just after its end. The start of November was used as the latest date from which imagery could be selected, since beyond this, mélangé in the fjord has been observed to freeze, causing the terminus to advance (Mortensen et al., 2011; Sole et al., 2011). The majority of images were acquired during September or October, though for 1993 and 2003 cloud-free images were only available for dates in August (30 August 1993 and 8 September 2003 respectively). No suitable images were available for the years 1988–1991 and 1998, meaning that annual resolution rates of terminus change were acquired for 1992–1997 and 1999–2012 (Table 1).

Where more than 1 year separated terminus observations, annually averaged rates of change were calculated. This provides a continuous record of the trends in behaviour, and inter-annual variability of KNS for the period spanning 1859–2012. This behaviour could then be directly compared to atmospheric and oceanic climate data.

Each terminus position was determined using an adaptation of the box method (Moon and Joughin, 2008; Howat and Eddy, 2011), called the Curvilinear Box Method (CBM; see Lea et al., 2014b, for details). This has a marked advantage over the centreline tracking or standard box methods as it is capable of accounting for changes in terminus geometry, while also accurately tracking changes in fjord orientation. Furthermore, the box used to calculate terminus change is always centred on the glacier/fjord centreline, which is also the flowline used for the numerical model. Consequently, terminus positions and observed distances of change derived using the CBM can be compared directly to model output.

2011

4 The TWG Model

The numerical model used is specifically designed to simulate the dynamics of TWGs along a flowband (Nick et al., 2010). It has been successful in replicating the dynamics of marine terminating outlets in both Greenland (e.g. Vieli and Nick, 2011; Nick et al., 2012; Lea et al., 2014a) and Antarctica (Jamieson et al., 2012, 2014), and has been used to make centennial timescale projections of the future contribution of Greenland's major TWG outlets to global sea level (Nick et al., 2013). The model accounts for basal, lateral and longitudinal shear stresses, and includes a robust treatment of grounding line dynamics (Pattyn et al., 2012). Bed topography data for the majority of the catchment are provided by Bamber et al. (2001), though the lower 40 km is generated using a mass continuity based bed reconstruction (Morlighem et al., 2011), validated by OIB/CRISIS flightlines (Gogineni et al., 2001). Where available, fjord bathymetry data are also used where KNS has retreated following its maximum (Weidick et al., 2012). Sensitivity analyses conducted by Lea et al. (2014a; their Fig. 10) for this bed configuration demonstrated that the model exhibits broadly comparable patterns of retreat behaviour where bed topography is varied within an uncertainty of ± 50 m.

A constant height vs. SMB relation is used to calculate SMB for the ablation zone of KNS (Eq. 1). This is derived from the average RACMO SMB model output for 1958–2007 (Van Angelen et al., 2013).

$$b(x) = 0.0018 \times h(x) - 2.693 \quad (1)$$

Where $b(x)$ = SMB for position x on the model flowline, and $h(x)$ = glacier elevation for position x on the flowline. Due to the tendency for over-estimation of accumulation in RACMO in this region (Van As et al., 2014), positive SMB values in the upstream section of the modelled glacier are prescribed to allow the glacier to maintain its contemporary elevation profile. Irrespective of this, SMB variability has previously been demonstrated to be of minimal importance to results of modelled TWG dynamics over the timescales that are being investigated (Lea et al., 2014a). The model is initialised

2012

The earliest images of KNS are from the 1850s and 1903. Both are taken from approximately the same position, with the terminus partially obscured by foreground topography (Weidick et al., 2012). The presence of medial moraines in each image demonstrates that KNS was confluent with AS. Lea et al. (2014a) quantified the terminus position uncertainty for the 1850s photograph using viewshed analysis. Similar analysis has been undertaken for the 1903 image, showing that the uncertainty in terminus position is the same as for the 1850s image (Fig. 3). The maximum terminus extents for both images are therefore located behind a headland corresponding to the ASM on the eastern side of the fjord (Figs. 1a and 3).

It is not currently possible to say when the ASM was attained from any observational evidence, only that it occurred sometime between 1859–1920. The climate anomalies for the period (compared to 1961–1990 baselines) show that air temperature (AT) and SST anomalies were, on average, antiphased for the period 1871–1903 (Fig. 4c and d), though AT and SST anomalies are in phase (negative/near-baseline) for 1903–1920. Conditions are therefore more likely to have been conducive for glacier advance during the latter period.

Terminus position was mapped directly for the remaining images, providing a record of 29 terminus positions spanning the period 1921–2012 (Figs. 1 and 4). The first direct terminus observation (1921) shows a slight retreat from the ASM. Subsequent to this, KNS retreated a total of 9.7 km at a non-uniform rate up to 2012, interrupted by short periods of readvance (Fig. 4a and b). Averaged retreat rates of -116 m a^{-1} are observed between 1921–1946, before a rapid retreat of 3.9 km within the 2 year period from 1946–1948 (Figs. 1a and 4). Between 1948–1968 KNS retreated on average by -97 m a^{-1} , before readvancing by $+60 \text{ m a}^{-1}$ up to 1979 (Fig. 4b). A terrestrial photograph taken in 1965 with the majority of the terminus obscured shows the termini of KNS and AS to be fully confluent.

The 1921–1968 period of sustained retreat was accompanied by positive average AT and SST anomalies (Fig. 4c and d). The highest AT anomalies occurred during the

2019

period 1928–1941, though the largest retreat (between 1946–1948) occurred during a comparatively less extreme period of positive AT and SST (Fig. 4).

From 1979 to 1987 KNS retreated by -658 m in total (-82 m a^{-1}), before readvancing by $+758 \text{ m}$ from 1987–1992 ($+152 \text{ m a}^{-1}$). Using the near complete 20 year annual record of terminus fluctuations from 1992–2012, KNS advanced for 4 out of 5 years between 1992–1997, followed by retreat in 11 out of 13 years from 1999–2012 at an average rate of -103 m a^{-1} . The latter included 8 annual retreats of $> 100 \text{ m}$, with the largest retreats occurring in 2004 (-438 m) and 2005 (-316 m). These periods of advance and retreat behaviour occurred during periods of in-phase negative and positive climate anomalies respectively.

Where temporal density of observations was high, terminus behaviour that was antiphased with the prevailing climate anomalies was also observed. Examples of this include a retreat of -626 m observed in 1995 during negative climate anomalies, while two terminus advances occur in 2008 and 2009 despite markedly positive AT and SST anomalies (Fig. 4). At annual resolution, the magnitude of terminus retreat/advance was also found to be unrelated to the magnitude of either climate anomaly for each particular year.

6 Model results

From a total of 1500 model runs conducted, 29 runs (1.9%) successfully replicated the observed dynamics of KNS according to the criteria outlined above (Fig. 5a). Following the initiation of climate forcing in 1871 (Fig. 5b and c), the results of each run are highly comparable up to 1884, with little modelled terminus change observed. Following this, for the period 1884 to ~ 1910 , 6 of the 29 runs (21%) show evidence of multi-annual terminus retreats and equivalent readvances of $> 750 \text{ m}$ with periodicities of 2–4 years. A further 7 runs (24%) show evidence of at least one short lived (< 5 year) oscillation in terminus position of $> 750 \text{ m}$ between 1884 to 1920. None of these model runs signifi-

2020

erage terminus change rates can be mitigated by averaging change over timescales up to, or greater than a decade. For example, extending the 1992–1997 average (51 ma^{-1} retreat) to cover the period 1987–1997 (91 ma^{-1} advance) provides a more representative impression of multi-annual terminus behaviour, since 5 out of the 6 observations
5 available show terminus advance. Interpreting absolute terminus change rate values should therefore be done with caution, and in most cases will be more representative of the average direction of terminus change rather than the absolute magnitude of annual change.

Taking into account uncertainties due to topographic controls on terminus stability,
10 observations of terminus change over a period of several years are more likely to allow a more accurate evaluation of a TWG’s response to climate forcings. However, for this study, deconvolving the relative importance of AT vs. SST in driving terminus change is difficult using observations alone, given that both climate drivers vary in phase for 1903–present. It could potentially be argued that AT is the primary driver of change,
15 since the 33 year period of positive anomaly SST from 1871–1903 had relatively little impact on the terminus stability of KNS. However, fjord geometry could also have been a significant factor stabilising the terminus during this time. Arguably this becomes less likely when it is considered that while SST was similar for the period 1921–1948, positive AT allowed KNS to retreat through the same section of fjord and through its
20 confluence with AS within 26 ± 1 years (Fig. 4). However, given the lack of certainty in terminus position between 1871–1920, it is not possible to robustly verify these arguments.

7.2 Implications of modelling

The observed terminus behaviour of KNS from 1921–2012 was successfully replicated
25 by 29 of 1500 model runs using surface runoff and SST records as drivers of terminus change. This demonstrates that the parameterisations used to scale these climate records to d_w and M respectively can successfully be used to simulate the observed pattern of behaviour of a tidewater glacier over centennial timescales. Where the ob-

2023

servational record is of sufficient detail to resolve inter-annual terminus fluctuations (1992–2012), the model does not replicate these. This is to be expected given (1) the flowband nature of the model and associated depth and width integrations over each grid cell, meaning that fluctuations of terminus configurations such as the creation of
5 calving bays cannot be replicated (e.g. Fig. 1b), (2) the uncertainty in fjord bathymetry and geometry potentially affecting relative terminus stability, and (3) the use of single terminus observations as notionally definitive indicators of annual terminus change, where the stochastic nature of calving and associated sub-annual terminus fluctuations make any direct one-to-one comparison of modelled results to annual resolution
10 observations inappropriate. Valid comparison of model results to observations should therefore only be attempted over multi-annual timescales where terminus dynamics within calving bays, sub-annual calving events and fine scale uncertainties in fjord topography become comparatively less significant.

For successful model runs, the interrelationships between the parameter values that
15 determine d_w and M sensitivity to the climate records also inform the relative importance of changes in atmospheric and oceanic forcing in driving terminus change. The lack of any significant relationship between α_1 and α_3 demonstrates that a change in model sensitivity to surface runoff is not offset by any change in model sensitivity to SST. Taken alone, this evidence indicates that either atmospheric forcing (via surface runoff) dominates oceanic forcing (via SST), or vice versa. However, the occurrence of
20 runs where α_3 does not significantly exceed 0 (i.e. where runs experience negligible M variability) demonstrate that the model can successfully reproduce observed behaviour with nearly no changes in oceanic forcing from year to year. Although some successful model runs did have significant inter-annual M variability (e.g. the maximum range of
25 M values for an entire 141 year model run was $0.76 \text{ km}^3 \text{ a}^{-1}$), each model run always requires significant atmospheric forcing variability to allow it to replicate observations.

The importance of oceanic forcing variability can therefore not be entirely discounted.

The model demonstrates that knowledge of atmospheric forcing variability (via runoff), without needing to vary oceanic forcing, can be sufficient to reproduce real-

istic patterns of observed glacier behaviour at KNS over the last century. However, the precise physical mechanism by which air temperature could drive observed change requires further investigation. For example, though a combination of modelled and empirically estimated runoff values have been used to drive changes in d_w to force the model, subglacial runoff variability is also known to drive rates of submarine melting at the terminus (Jenkins, 2011; Xu et al., 2012; Sciascia et al., 2013). Therefore we do not rule out that the centennial behaviour observed could also be explained by calving driven by seasonal changes in submarine melt rates, that are in turn a function of subglacial runoff (e.g. Sciascia et al., 2013).

The relative insensitivity to changes in oceanic forcing is not necessarily surprising given the hydrographic setting of KNS – located at the end of a > 100 km long fjord system that is thought to be largely insulated from changes in ocean conditions due to the presence of a shallow sill at its entrance (Mortensen et al., 2011, 2013). This has previously been used to suggest that recent changes in ocean conditions (e.g. Straneo and Heimbach, 2013) have not affected the dynamics of KNS significantly (Straneo et al., 2012). The results presented here are therefore compatible with this argument.

The over-estimation of terminus retreat by 2012 of every successful run is thought to result from the poor knowledge of fjord width geometry beyond the contemporary glacier terminus. Upstream of the 2012 terminus, the lateral ice margins are used to define model glacier width, leading to a likely over-estimation of the prescribed fjord width. The divergence between the actual and prescribed fjord width is therefore likely to increase upglacier, increasing the likelihood of model error in this area. This explains why significant divergence from the observational record only occurs once the modelled terminus has retreated ~ 1.5 km beyond the 2012 terminus. Any attempt at modelling the future fluctuations of KNS will therefore require both improvements to subglacial topography estimates and comprehensive assessments of fjord width uncertainties as part of any predictions.

2025

8 Conclusions

Utilising multiple lines of evidence, it has been possible to reconstruct terminus fluctuations of KNS from 1859–2012. This study therefore completes the record of terminus fluctuations of KNS from its LIAMax, in 1761, up to the present (Lea et al., 2014a), providing one of the longest, and most detailed records of observed TWG change in Greenland. Results from numerical modelling show that the fluctuations of KNS can be simulated through parameterisations that link surface runoff to a crevasse water depth based calving criterion. Changes in both/either crevasse water depth and/or runoff driven rates of submarine melt are therefore suggested as potential drivers of observed change. Although ocean driven changes in submarine melt rates are not always required for the model to replicate the observed length variations of KNS, results do not allow their importance to be discounted entirely.

Observations of KNS show it to respond in phase with AT and SST anomalies over multi-annual to decadal timescales from at least 1921–2012. However, where inter-annual comparisons to AT and SST are possible (1992–2012), climatically anti-phased terminus fluctuations are observed. This highlights the inherent noisiness of terminus response over short timescales, the potential importance of antecedence, and the dangers of using similarly short calibration periods for predictive modelling efforts.

Results from numerical modelling successfully capture the terminus dynamics of KNS over multi-annual to decadal timescales, though not precise inter-annual fluctuations. This is due to a combination of uncertainties in fjord topography, and the approximations inherent to the depth and width integrations associated with using a one-dimensional flow-band model.

Nevertheless, this study demonstrates that simple flow-band numerical models of tidewater glaciers can be used to capture TWG dynamics over centennial timescales. This provides validation that these models can be useful tools for both palaeo- and contemporary/prognostic modelling efforts. However, the primary challenge to their use as predictive tools remain the accurate definition of subglacial topography and fjord

2026

width, which exert dominant controls on modelled glacier stability. Any future efforts at prognostic modelling of TWGs should therefore seek to account for these uncertainties in addition to those associated with sensitivity to climate forcing.

5
10 *Acknowledgements.* RACMO2.1 data were provided by Jan van Angelen and Michiel van den Broeke, IMAU, Utrecht University. MAR v3.2 data used for runoff calculations were provided by Xavier Fettweis, Department of Geography, University of Liège. The photogrammetric DEM used in Figs. 1 and 3 was provided by Kurt H. Kjær, Centre for GeoGenetics, University of Copenhagen. This research was financially supported by J.L.'s PhD funding, NERC grant number: NE/I528742/1. Support for F.M.N. was provided by the Conoco-Phillips/Lundin Northern Area Program CRIOS project (Calving Rates and Impact on Sea Level).

References

- Alley, R. B., Andrews, J. T., Brigham-Grette, J., Clarke, G. K. C., Cuffey, K. M., Fitzpatrick, J. J., Funder, S., Marshall, S. J., Miller, G. H., Mitrovica, J. X., Muhs, D. R., Otto-Bliesner, B. L., Polyak, L., and White, J. W. C.: History of the Greenland Ice Sheet: paleoclimatic insights, *Quaternary Sci. Rev.*, 29, 1728–1756, doi:10.1016/j.quascirev.2010.02.007, 2010.
- 15 Bamber, J. L., Layberry, R. L., and Gogineni, S. P.: A new ice thickness and bed data set for the Greenland ice sheet: 1. Measurement, data reduction, and errors, *J. Geophys. Res.*, 106, 33773–33780, doi:10.1029/2001JD900054, 2001.
- Bevan, S. L., Luckman, A. J., and Murray, T.: Glacier dynamics over the last quarter of a century at Helheim, Kangerdlugssuaq and 14 other major Greenland outlet glaciers, *The Cryosphere*, 6, 923–937, doi:10.5194/tc-6-923-2012, 2012.
- 20 Brede, N.: Skizze Kaart over Vestkysten af Grønland fra Arsuk til Holsteensborg, KBK Netpublikation DK003200, Copenhagen, 1866.
- Bjørk, A. A., Kjær, K. H., Korsgaard, N. J., Khan, S. A., Kjeldsen, K. K., Andresen, C. S., Larsen, N. K., and Funder, S.: An aerial view of 80 years of climate-related glacier fluctuations in southeast Greenland, *Nat. Geosci.*, 5, 427–432, doi:10.1038/ngeo1481, 2012.
- Bruun, D.: Oversigt over Norburuiner i Godthaab og Frederikshaab Distrikter, *Meddelelser om Grønland*, 56, 55–147, 1917.
- Cappelen, J.: Greenland-DMI Historical Climate Data Collection 1873–2011, Technical Report 30 12-04, Danish Meteorological Institute, Copenhagen, 2012.
- 2027

- Colgan, W., Pfeffer, W. T., Rajaram, H., Abdalati, W., and Balog, J.: Monte Carlo ice flow modeling projects a new stable configuration for Columbia Glacier, Alaska, c. 2020, *The Cryosphere*, 6, 1395–1409, doi:10.5194/tc-6-1395-2012, 2012.
- Cook, S., Zwinger, T., Rutt, I. C., O'Neel, S., and Murray, T.: Testing the effect of 5 water in crevasses on a physically based calving model, *Ann. Glaciol.*, 53, 90–96, doi:10.3189/2012AoG60A107, 2012.
- Cook, S., Rutt, I. C., Murray, T., Luckman, A., Selmes, N., Goldsack, A., and Zwinger, T.: Modelling environmental influences on calving at Helheim Glacier, East Greenland, *The Cryosphere Discuss.*, 7, 4407–4442, doi:10.5194/tcd-7-4407-2013, 2013.
- 10 Csatho, B., Schenk, T., Van der Veen, C. J., and Krabill, W. B.: Intermittent thinning of Jakobshavn Isbræ, West Greenland, since the Little Ice Age, *J. Glaciol.*, 54, 131–144, doi:10.3189/002214308784409035, 2008.
- Rink, H.: Kyststrækning fra Frederikshåb i syd til Napasaq i nord, KBK Netpublikation RI000029, Copenhagen, 1866.
- 15 Fettweis, X., Tedesco, M., van den Broeke, M., and Ettema, J.: Melting trends over the Greenland ice sheet (1958–2009) from spaceborne microwave data and regional climate models, *The Cryosphere*, 5, 359–375, doi:10.5194/tc-5-359-2011, 2011.
- Gogineni, S., Tammana, D., Braaten, D., Leuschen, C., Akins, T., Legarsky, J. K., Kanagaratnam, P., Stiles, J., Allen, C., and Jezek, K.: Coherent radar ice thickness measurements over the Greenland ice sheet, *J. Geophys. Res.*, 106, 33761–33772, doi:10.1029/2001JD900183, 2001.
- Hanna, E., Cappelen, J., Fettweis, X., Huybrechts, P., Luckman, A., and Ribergaard, M. H.: Hydrologic response of the Greenland ice sheet: the role of oceanographic warming, *Hydrol. Process.*, 23, 7–30, doi:10.1002/hyp.7090, 2009.
- 25 Howat, I. M. and Eddy, A.: Multi-decadal retreat of Greenland's marine-terminating glaciers, *J. Glaciol.*, 57, 389–396, doi:10.3189/002214311796905631, 2011.
- Hvidegaard, S. M., Sorensen, L. S., and Forsberg, R.: ASTER GDEM validation using LiDAR data over coastal regions of Greenland, *Remote Sensing Letters*, 3, 85–91, doi:10.1080/01431161.2010.527389, 2012.
- 30 Jamieson, S. S. R., Vieli, A., Livingstone, S. J., Cofaigh, C. Ó., Stokes, C., Hillenbrand, C. D., and Dowdeswell, J. A.: Ice-stream stability on a reverse bed slope, *Nat. Geosci.*, 5, 799–802, doi:10.1038/ngeo1600, 2012.

- Jamieson, S. S. R., Vieli, A., Cofaigh, C. Ó, Stokes, C. R., Livingstone, S. J., and Hillenbrand, C.-D.: Understanding controls on rapid ice-stream retreat during the last deglaciation of Marguerite Bay, Antarctica, using a numerical model, *J. Geophys. Res.*, 119, 247–263, doi:10.1002/2013JF002934, 2014.
- 5 Jenkins, A.: Convection-driven melting near the grounding lines of ice shelves and tidewater glaciers, *J. Phys. Oceanogr.*, 41, 2279–2294, doi:10.1175/JPO-D-11-03.1, 2011.
- Jensen, J. A. D.: Vestkysten af Grønland fra Arsuk til Holstensborg 61° til 67° N, KBK Netpublikation, DK003198, Copenhagen, 1885
- Joughin, I., Smith, B. E., Howat, I. M., Scambos, T., and Moon, T.: Greenland flow variability from ice-sheet-wide velocity mapping, *J. Glaciol.*, 56, 415–430, doi:10.3189/002214310792447734, 2010.
- 10 Kleinschmidt, S.: Godthåbs distrikt (hertil en Navneliste), KBK Netpublikation RI000074, Copenhagen, 1859.
- Lea, J. M., Mair, D. W. F., Nick, F. M., Rea, B. R., Weidick, A., Kjær, K., Morlighem, M., van As, D., and Schofield, J. E.: Terminus-driven retreat of a major southwest Greenland tidewater glacier during the early 19th century: insights from glacier reconstructions and numerical modelling, *J. Glaciol.*, 220, 333–344, doi:10.3189/2014JoG13J163, 2014a.
- 15 Lea, J. M., Mair, D. W. F., and Rea, B. R.: Evaluation of existing and new methods of tracking glacier terminus change, *J. Glaciol.*, 220, 322–332, doi:10.3189/2014JoG13J061, 2014b.
- Morlighem, M., Rignot, E., Seroussi, H., Larour, E., Ben Dhia, H., and Aubry, D.: A mass conservation approach for mapping glacier ice thickness, *Geophys. Res. Lett.*, 38, L19503, doi:10.1029/2011GL048659, 2011.
- McFadden, E. M., Howat, I. M., Joughin, I., Smith, B. E., and Ahn, Y.: Changes in the dynamics of marine terminating outlet glaciers in west Greenland (2000–2009), *J. Geophys. Res.*, 116, F02022, doi:10.1029/2010JF001757, 2011.
- 25 Moon, T. and Joughin, I.: Changes in ice front position on Greenland's outlet glaciers from 1992 to 2007, *J. Geophys. Res.*, 113, F02022, doi:10.1029/2007JF000927, 2008.
- Mortensen, J., Lennert, K., Bendtsen, J., and Rysgaard, S.: Heat sources for glacial melt in a sub-Arctic fjord (Godthåbsfjord) in contact with the Greenland Ice Sheet, *J. Geophys. Res.*, 116, C01013, doi:10.1029/2010JC006528, 2011.
- 30 Mortensen, J., Bendtsen, J., Motyka, R. J., Lennert, K., Truffer, M., Fahnestock, M., and Rysgaard, S.: On the seasonal freshwater stratification in the proximity of fast-flowing

2029

- tidewater outlet glaciers in a sub-Arctic sill fjord, *J. Geophys. Res.*, 118, 1382–1395, doi:10.1002/jgrc.20134, 2013.
- Murray, T., Scharrer, K., James, T. D., Dye, S. R., Hanna, E., Booth, A. D., Selmes, N., Luckman, A., Hughes, A. L. C., Cook, S., and Huybrechts, P.: Ocean regulation hypothesis for glacier dynamics in southeast Greenland and implications for ice sheet mass changes, *J. Geophys. Res.*, 115, F03026, doi:10.1029/2009JF001522, 2010.
- 5 Nansen, F.: *The First Crossing of Greenland*, Longmans, London, 1890.
- Nick, F. M., Van der Veen, C. J., Vieli, A., and Benn, D. I.: A physically based calving model applied to marine outlet glaciers and implications for the glacier dynamics, *J. Glaciol.*, 56, 781–794, doi:10.3189/002214310794457344, 2010.
- 10 Nick, F. M., Luckman, A., Vieli, A., Van der Veen, C. J., Van As, D., Van de Wal, R. S. W., Pattyn, F., Hubbard, A. L., and Floricioiu, D.: The response of Petermann Glacier, Greenland, to large calving events, and its future stability in the context of atmospheric and oceanic warming, *J. Glaciol.*, 58, 229–239, doi:10.3189/2012JoG11J242, 2012.
- 15 Nick, F. M., Vieli, A., Andersen, M. L., Joughin, I., Payne, A., Edwards, T. L., Pattyn, F., van de Wal, R. S.: Future sea-level rise from Greenland's main outlet glaciers in a warming climate, *Nature*, 497, 235–238, doi:10.1038/nature12068, 2013.
- Pattyn, F., Schoof, C., Perichon, L., Hindmarsh, R. C. A., Bueler, E., de Fleurian, B., Durand, G., Gagliardini, O., Gladstone, R., Goldberg, D., Gudmundsson, G. H., Huybrechts, P., Lee, V., Nick, F. M., Payne, A. J., Pollard, D., Rybak, O., Saito, F., and Vieli, A.: Results of the Marine Ice Sheet Model Intercomparison Project, MISMIP, *The Cryosphere*, 6, 573–588, doi:10.5194/tc-6-573-2012, 2012.
- 20 Poulsen, J.: *Godthåb Kommune*, KBK Netpublikation RI000059, Copenhagen, 1860.
- Rayner, N. A., Parker, D. E., Horton, E. B., Folland, C. K., Alexander, L. V., Rowell, D. P., Kent, E. C., and Kaplan, A.: Global analyses of sea surface temperature, sea ice, and night marine air temperature since the late nineteenth century, *J. Geophys. Res.*, 108, 4407, doi:10.1029/2002JD002670, 2003.
- Rignot, E., Fenty, I., Menemenlis, D., and Xu, Y.: Spreading of warm ocean waters around Greenland as a possible cause for glacier acceleration, *Ann. Glaciol.*, 53, 257–266, doi:10.3189/2012AoG60A136, 2012.
- 30 Russell, A.: Farms and churches of the medieval Norse settlement in Greenland, *Meddelelser om Grønland*, 89, 342 pp., 1941.

2030

- Sciascia, R., Straneo, F., Cenedese, C., and Heimbach, P.: Seasonal variability of submarine melt rate and circulation in an East Greenland fjord, *J. Geophys. Res.*, 118, 2492–2506, doi:10.1002/jgrc.20142, 2013.
- 5 Sole, A. J., Mair, D. W. F., Nienow, P. W., Bartholomew, I. D., King, M. A., Burke, M. J., and Joughin, I.: Seasonal speedup of a Greenland marine-terminating outlet glacier forced by surface melt-induced changes in subglacial hydrology, *J. Geophys. Res.*, 116, F03014, doi:10.1029/2010JF001948, 2011.
- Straneo, F. and Heimbach, P.: North Atlantic warming and the retreat of Greenland's outlet glaciers, *Nature*, 504, 36–43, doi:10.1038/nature12854, 2013.
- 10 Straneo, F., Hamilton, G. S., Sutherland, D. A., Stearns, L. A., Davidson, F., Hammill, M. O., Stenson, G. B., and Rosing-Asvid, A.: Rapid circulation of warm subtropical waters in a major glacial fjord in East Greenland, *Nat. Geosci.*, 3, 182–186, doi:10.1038/ngeo764, 2010.
- Straneo, F., Sutherland, D. A., Holland, D., Gladish, C., Hamilton, G. S., Johnson, H. L., Rignot, E., Xu, Y., and Koppes, M.: Characteristics of ocean waters reaching Greenland's glaciers, *Ann. Glaciol.*, 53, 202–210, doi:10.3189/2012AoG60A059, 2012.
- 15 Taurisano, A., Bøggild, C. E., and Karlsen, H. G.: A century of climate variability and climate gradients from coast to ice sheet in West Greenland, *Geogr. Ann. A*, 86, 217–224, doi:10.1111/j.0435-3676.2004.00226.x, 2004.
- Van Angelen, J. H., van den Broeke, M. R., Wouters, B., and Lenaerts, J. T. M.: Contemporary (1960–2012) evolution of the climate and surface mass balance of the Greenland ice sheet, *Surv. Geophys.*, doi:10.1007/s10712-013-9261-z, 2013.
- 20 Van As, D., Andresen, M. L., Petersen, D., Fettweis, X., van Angelen, J. H., Lenearts, J. T. M., van den Broeke, M. R., Lea, J. M., Bayou, N., Bøggild, C. E., Ahlstrøm, A. P., and Steffen, K.: Increasing meltwater discharge from the Nuuk region of the Greenland ice sheet and implications for mass balance (1960–2012), *J. Glaciol.*, 220, 314–322, 2014.
- 25 Van den Broeke, M., Bamber, J., Ettema, J., Rignot, E., Schrama, E., van de Berg, W. J., van Meijgaard, E., Velicogna, I., and Wouters, B.: Partitioning recent Greenland mass loss, *Science*, 326, 984–986, doi:10.1126/science.1178176, 2009.
- Vieli, A. and Nick, F. M.: Understanding and modelling rapid dynamic changes of tidewater outlet glaciers: issues and implications, *Surv. Geophys.*, 32, 437–458, doi:10.1007/s10712-011-9132-4, 2011.
- 30

2031

- Vinther, B. M., Andersen, K. K., Jones, P. D., Briffa, K. R., and Cappelen, J.: Extending Greenland temperature records into the late eighteenth century, *J. Geophys. Res.*, 111, D11105, doi:10.1029/2005JD006810, 2006.
- Weidick, A. and Citterio, M.: The ice-dammed lake Isvand, West Greenland, has lost its water, *J. Glaciol.*, 57, 186–188, doi:10.3189/002214311795306600, 2011.
- 5 Weidick, A., Bennike, O., Citterio, M., and Nørgaard-Pedersen, N.: Neoglacial and Historical Glacier Changes around Kangarsuneq Fjord in Southern West Greenland, Geological Survey of Denmark and Greenland, Copenhagen, 2012.
- Xu, Y., Rignot, E., Menemenlis, D., and Koppes, M.: Numerical experiments on subaqueous melting of Greenland tidewater glaciers in response to ocean warming and enhanced subglacial discharge, *Ann. Glaciol.*, 53, 229–234, doi:10.3189/2012AoG60A139, 2012.
- 10

2032

Table 1. List of terminus observations and acquisition dates.

Acquisition date	Observation type	Source
1850s	Terrestrial photo'	H. Rink (in Weidick et al., 2012)
1859	Map	Kleinschmidt (1859)
1860	Map	Poulsen (1860)
1866	Map	Rink (1866)
1866	Map	Falbe (1866)
1885	Map	Jensen (1885)
1880s?	Sketch (after photo')	Nansen (1890)
1903	Terrestrial photo'	J. Møller in Bruun (1917)
1921	Terrestrial photo'	A. Nissen in Weidick et al. (2012)
1932	Terrestrial photo'	A. Roussell in Roussell (1941)
27 Aug 1936	Oblique photo'	Weidick et al. (2012)
10 Aug 1946	Oblique photo'	Weidick et al. (2012)
20 Aug 1948	Oblique photo'	Weidick et al. (2012)
21 Jun 1965	Terrestrial photo'	Weidick et al. (2012)
16 Aug 1968	Aerial photo'	USGS
15 Sep 1979	Terrestrial photo'	Weidick et al. (2012)
15 Sep 1987	Satellite	Landsat
19 Sep 1992	Satellite	Landsat
30 Aug 1993	Satellite	Landsat
18 Sep 1994	Satellite	Landsat
14 Oct 1995	Satellite	Landsat
14 Sep 1996	Satellite	Landsat
1 Sep 1997	Satellite	Landsat
15 Sep 1999	Satellite	Landsat
18 Sep 2000	Satellite	Landsat
22 Oct 2001	Satellite	Landsat
23 Sep 2002	Satellite	Landsat
9 Aug 2003	Satellite	Landsat
12 Sep 2004	Satellite	Landsat
24 Sep 2005	Satellite	Landsat
18 Sep 2006	Satellite	Landsat
27 Sep 2007	Satellite	Landsat
23 Sep 2008	Satellite	Landsat
19 Sep 2009	Satellite	Landsat
13 Sep 2010	Satellite	Landsat
16 Sep 2011	Satellite	Landsat
18 Sep 2012	Satellite	Landsat

2033

Table 2. List of parameters and constants used for running the model.

Parameter/Constant	Value
Ice density – ρ_i	900 kg m ⁻³
Meltwater density – ρ_w	1000 kg m ⁻³
Proglacial water body density – ρ_p	1028 kg m ⁻³
Gravitational acceleration – g	9.8 m s ⁻²
Friction exponent – m	3
Friction parameters – μ and λ	1
Glen's flow law exponent – n	3
Glen's flow law coefficient – A	4.5×10^{-17} Pa ⁻³ a ⁻¹
Grid size	~ 250 m
Time step	0.005 a

2034

Table 3. Pearson correlation coefficient values for tuning parameters of successful model runs ($n = 29$). Correlation coefficients with p values < 0.05 are highlighted in bold.

	α_1	α_2	α_3	M_{base}
α_1	–	–0.92	0.29	–0.47
α_2	–0.92	–	–0.46	0.29
α_3	0.29	–0.46	–	–0.43
M_{base}	–0.47	0.29	–0.43	–

2035

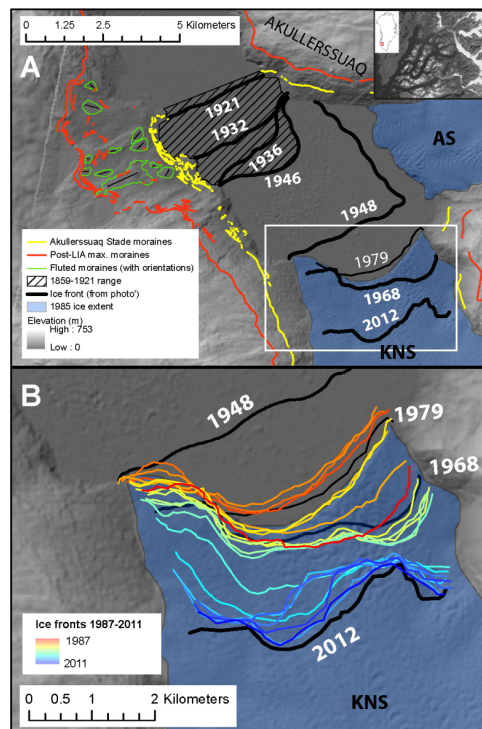


Fig. 1. Diagrams showing the site location (inset), terminus positions and geomorphology plotted on a hillshaded mosaic of a stereophotogrammetrically derived digital elevation model (DEM) from images acquired in 1985, and ASTER GDEM (Hvidegaard et al., 2012). **(A)** Termini and geomorphology for 1859–2012, with ASM limits delineated in yellow, and **(B)** a detailed view of termini for the period 1948–2012.

2036

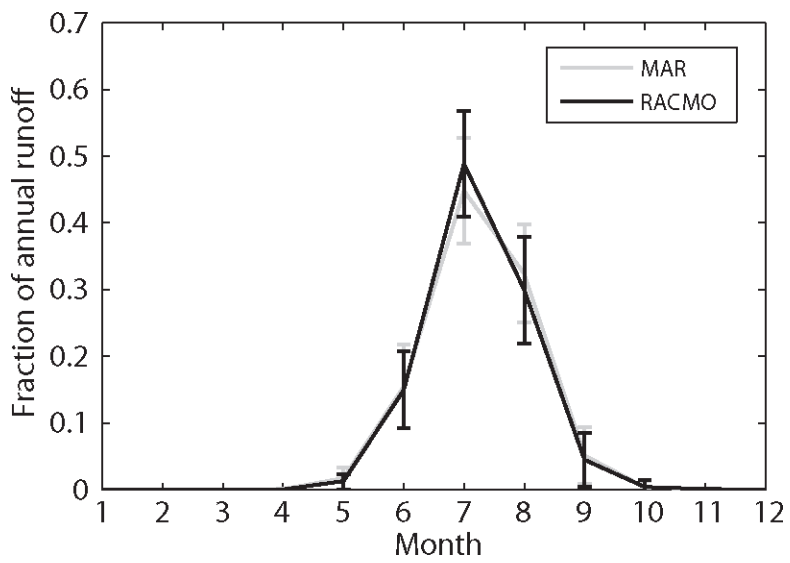


Fig. 2. Fraction of annual runoff occurring for each month as given by MAR and RACMO2 SMB models for KNS and AS between 1960–2012 (Van As et al., 2014). Error bars are given to 2 standard deviations.

2037

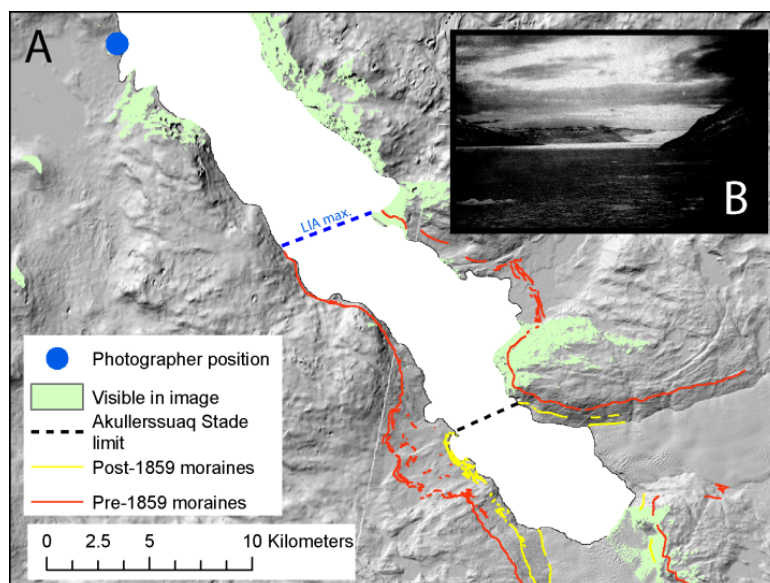


Fig. 3. Reconstructed photographer position showing (A) the area that would be observable in the photograph shown in (B) that was acquired in 1903.

2038

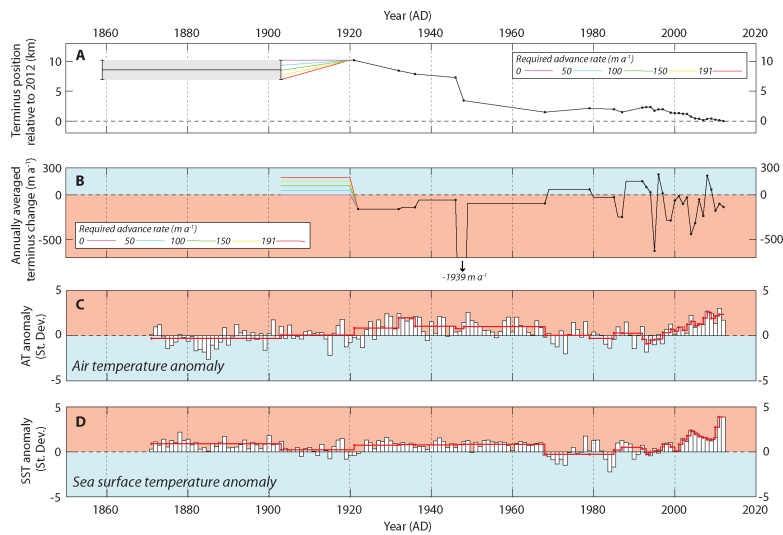


Fig. 4. (A) Terminology change relative to the 2012 terminus position. Uncertainty in terminus position for 1859–1903 highlighted in grey, with a range of potential advance rates for 1903–1920 indicated. These range from a minimum of no change (0 m a^{-1}) to a maximum possible advance rate of 191 m a^{-1} . (B) Annually averaged rates of terminus change between observations (black dots). Includes terminus advance rates described for 1903–1921 terminus change indicated on A. (C) Summer ATA (June, July, August) at annual resolution (white bars), and red line showing the averaged ATA between terminus observations (Cappelen et al., 2012; Vinther et al., 2006). (D) Annual SSTA for the area 61° to 65° N 51° to 56° W at annual resolution (white bars) and red line showing the averaged SSTA between terminus observations (Rayner et al., 2003).

2039

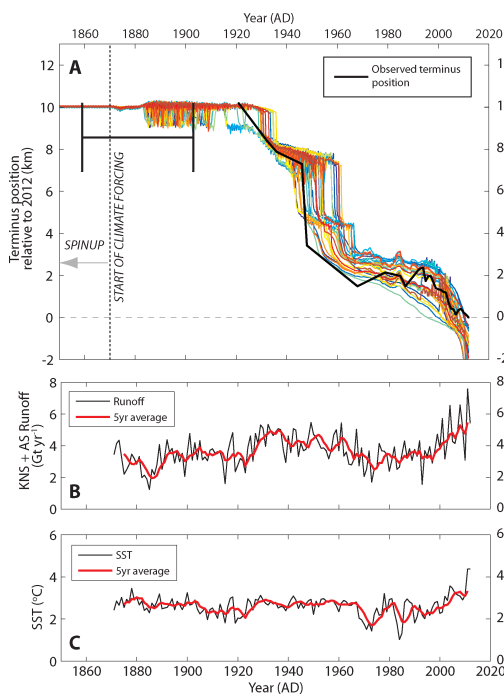


Fig. 5. (A) Evolution of terminus position for model runs (coloured lines) determined to be successful according to the criteria outlined in the text, with observed terminus position also plotted (bold black line, with positions between observations linearly interpolated). (B) Combined KNS and AS runoff volume estimates for 1871–2012 that are used to drive the model (5 year moving average also plotted in red). (C) Absolute annual SST estimates used to drive the model from Rayner et al. (2003) for the area 61° to 65° N and 51° to 56° W (5 year moving average also plotted in red).

2040

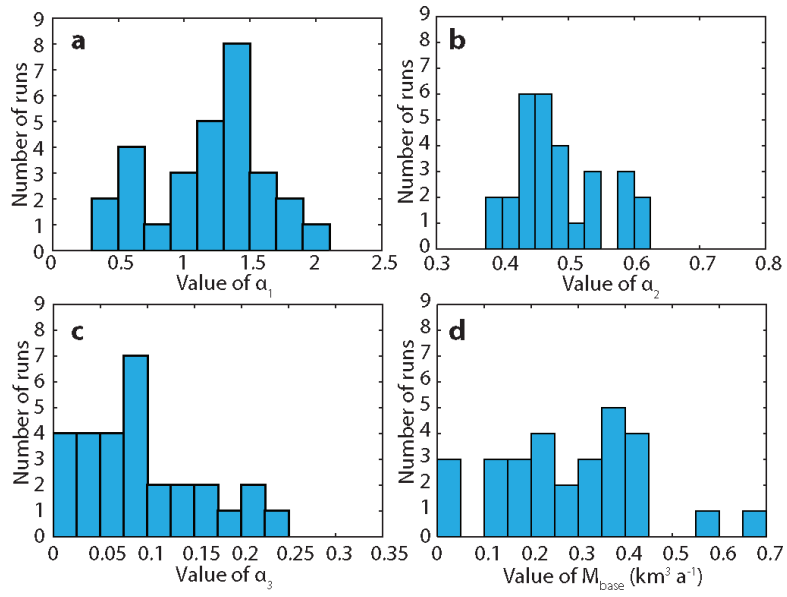


Fig. 6. The distribution of the tuning parameters **(a)** α_1 (bin width = 0.2), **(b)** α_2 (bin width = 0.025), **(c)** α_3 (bin width = 0.025), and **(d)** M_{base} (bin width = $0.05 \text{ km}^3 \text{ a}^{-1}$) for successful runs as defined by the criteria outlined in the text. Minimum and maximum x-axis values represent the full range of values tested within the 1500 model runs.

1 **Fluctuations of a Greenlandic tidewater glacier driven by**
2 **changes in atmospheric forcing: observations and**
3 **modelling of Kangiata Nunaata Sermia, 1859-present.**

4
5 **J. M. Lea^{1*}, D. W. F. Mair¹, F. M. Nick^{2,3}, B. R. Rea¹, D. van As⁴, M. Morlighem⁵,**
6 **P. W. Nienow⁶, A. Weidick⁴**

7
8 [1]{Department of Geography and the Environment, University of Aberdeen,
9 Elphinstone Road, AB24 3UF, UK}

10 [2]{The University Centre in Svalbard (UNIS), PO Box 156, NO-9171 Longyearbyen,
11 Norway}

12 [3]{Centre for Ice and Climate, Niels Bohr Institute, University of Copenhagen,
13 Copenhagen, 2100, Denmark}

14 [4]{Geological Survey of Denmark and Greenland (GEUS), Copenhagen, Denmark}

15 [5]{University of California, Irvine, Department of Earth System Science, Croul Hall,
16 Irvine, CA 92697-3100, USA}

17 [6]{Department of Geography, University of Edinburgh, Drummond Street,
18 Edinburgh, EH8 9XP, UK}

19 [*]{Now at: Department of Geography and Quaternary Geology, Stockholm
20 University, SE-106 91, Stockholm, Sweden}

21
22 Correspondence to: J. M. Lea (james.lea@natgeo.su.se)

23
24 **Abstract**

25 Many tidewater glaciers in Greenland are known to have undergone significant
26 retreat during the last century following their Little Ice Age maxima. Where it is
27 possible to reconstruct glacier change over this period, they provide excellent
28 records for comparison to climate records, and calibration/validation for numerical
29 models. These glacier change records therefore allow tests of numerical models that
30 seek to simulate tidewater glacier behaviour over multi-decadal to centennial
31 timescales. Here we present a detailed record of behaviour from Kangiata Nunaata

1 Sermia (KNS), SW Greenland, between 1859-2012 and compare it against available
2 oceanographic and atmospheric temperature data between 1871-2012. We also use
3 these records to evaluate the ability of a well-established one-dimensional flow-band
4 model to replicate behaviour for the observation period. The record of terminus
5 change demonstrates that KNS has advanced/retreated in phase with atmosphere
6 and ocean climate anomalies averaged over multi-annual to decadal timescales.
7 Results from an ensemble of model runs demonstrate that observed dynamics can
8 be replicated. Model runs that provide a reasonable match to observations always
9 require a significant atmospheric forcing component, but do not necessarily require
10 an oceanic forcing component. Although the importance of oceanic forcing cannot be
11 discounted, these results demonstrate that changes in atmospheric forcing are likely
12 to be a primary driver of the terminus fluctuations of KNS from 1859-2012. We
13 propose that the detail and length of the record presented makes KNS an ideal site
14 for model validation exercises investigating links between climate, calving rates and
15 tidewater glacier dynamics.

16
17

18 **1. Introduction**

19 Calving from tidewater glaciers (TWGs) presently accounts for up to 50% of the
20 mass loss from the Greenland Ice Sheet (Van den Broeke et al., 2009). Determining
21 controls on tidewater glacier dynamics over decadal to centennial timescales is
22 crucial to understanding their contribution to sea level in a warming climate (Alley et
23 al., 2010; Vieli and Nick, 2011). The ability to achieve this in Greenland has been
24 restricted in part by the relative lack of TWG terminus observations prior to the
25 satellite age, and evidence of terminus locations being spread across a disparate
26 array of sources. However, the synthesis of these sources has previously allowed
27 multi-decadal to centennial records of TWG glacier behaviour to be reconstructed
28 (e.g. Csatho et al., 2008; Bjørk et al., 2012; Weidick et al., 2012).

29 Such records provide potentially excellent calibration and validation records
30 for numerical modelling efforts (Viel and Nick, 2011). That is to say, numerical
31 models that are capable of replicating observed terminus behaviour over decadal to
32 centennial timescales will be better placed to predict the future behaviour of a TWG
33 over similar timescales. Despite this, there remain few examples of modelling efforts

1 that have attempted to calibrate their results against multi-decadal observational
2 records (e.g. Colgan et al., 2012). The ability of most numerical models to replicate
3 dynamics over such timescales using realistic inputs therefore remains largely
4 untested.

5 By undertaking calibration/validation exercises, the sensitivity of the terminus
6 to different climatic forcing can also be evaluated (e.g. Nick et al., 2013; Cook et al.,
7 2013; Lea et al., 2014a). This is achieved by comparing the sensitivity of a modelled
8 glacier to climate forcing against observations (Nick et al., 2013). With a knowledge
9 of realistic ranges of forcing, this allows evaluation of the relative importance of each
10 in contributing to the observed TWG behaviour.

11 Changes in oceanic forcing are significant drivers of TWG retreat in
12 Greenland (Murray et al., 2010; Straneo et al., 2010; Rignot et al., 2012), but their
13 relative importance between glaciers appears to be dependent on geographical
14 location, glacier geometry (Nick et al., 2013), and potentially fjord connectivity with
15 the open ocean (Straneo et al., 2012). Model based studies have also helped to
16 demonstrate the sensitivity of some major outlet glaciers to air temperature changes
17 (via enhanced runoff increasing crevasse water depth; Nick et al., 2013; Cook et al.,
18 2013).

19 Where multi-decadal to centennial timescale climate data exist alongside
20 records of terminus position, these provide the potential for robust evaluation of both
21 numerical models and the importance of different drivers of TWG terminus change.
22 In this study we aim to (1) reconstruct the fluctuations of Kangiata Nunaata Sermia
23 (KNS), SW Greenland from 1859-present, coinciding with the availability of climate
24 records, (2) use these data to evaluate the ability of a well-established climate-driven
25 numerical ice-flow model, to replicate its dynamics, and (3) in conjunction with fjord
26 topography data, assess controls on the terminus stability of KNS over multi-decadal
27 to centennial timescales.

28

29 **2. Field site and climate data**

30 KNS is the largest TWG on the west coast of Greenland, south of Jakobshavn Isbræ
31 (Figure 1; Van As et al., 2014). It is known to have undergone significant retreat
32 since its Little Ice Age maximum (Weidick et al., 2012), retreating a total of 22.6 km,
33 with at least 12 km of this retreat occurring prior to 1859 when climate forcing data
34 are unavailable (Lea et al., 2014a). It is situated ~100 km inland from Nuuk at the

1 head of Godthåbsfjord, and currently has a calving flux of $\sim 6 \text{ km}^3 \text{ a}^{-1}$ (Van As et al.,
2 2014).

3 A continuous record of mean monthly air temperature is available at Nuuk
4 from 1866-present (Vinther et al., 2006; Cappelen et al., 2012). Temperatures at
5 Nuuk are known to be strongly correlated with those near to the terminus region of
6 KNS throughout the year (Taurisano et al., 2004). For this reason, we take the Nuuk
7 record as an indicator of the atmospheric forcing at KNS.

8 As with all TWGs around Greenland, there are no long observational records
9 of fjord water temperatures adjacent to KNS, though detailed hydrographic studies of
10 the fjord have been undertaken recently (Mortensen et al., 2011; 2013). A shallow
11 $\sim 80 \text{ m}$ sill at the entrance to Godthåbsfjord at Nuuk has been suggested to limit the
12 connectivity of the fjord to warm ocean waters at depth. In fjords where shallow sills
13 do not exist, the incursion of these warm ocean waters are thought to have
14 significantly affected the stability of TWGs (Rignot et al., 2012; Straneo et al., 2012).
15 The presence of the shallow sill in Godthåbsfjord also results in significant tidal
16 mixing at the fjord entrance, allowing sea surface waters to be incorporated at depth,
17 which are then advected into the fjord (Mortensen et al., 2011). These intermediate
18 level mixed waters have been proposed to significantly influence the energy
19 available for submarine melting at the termini of the TWGs in Godthåbsfjord
20 (Mortensen et al., 2013).

21 Due to the impact of surface waters near the fjord entrance on the energy
22 balance of the fjord (Mortensen et al., 2011; 2013), and the potentially restricted
23 influence of warm coastal currents at depth (Straneo et al., 2012), we suggest that
24 sea surface temperatures (SSTs) provide a good indicator of the relative
25 oceanographic forcing affecting KNS. Such data have also been used previously to
26 interrogate the role of oceanographic forcing on TWG stability where observations at
27 depth are unavailable (e.g. McFadden et al., 2011; Bevan et al., 2012). The
28 HadISST1 $1^\circ \times 1^\circ$ dataset provides SST estimates for the period 1871-present
29 (Rayner et al., 2003), with annual averages for the area immediately offshore from
30 Nuuk (62° to 64° N 51° to 53° W) used as an indicator of oceanographic conditions
31 affecting Godthåbsfjord. Although the data used will in part be based on interpolation
32 of observations (especially in the earlier part of the record), the data have been
33 validated for west Greenland against independent records back to 1875 (Hanna et

1 al., 2009). This therefore provides confidence in the results obtained from the
2 HadISST1 dataset.

3

4 **3. Glacier reconstruction data**

5 A combination of geomorphology, maps, photography (ground-based, oblique-aerial,
6 and vertical aerial images), and satellite imagery are used to reconstruct the
7 terminus dynamics of KNS. By 1859 KNS is known to have retreated between 12-15
8 km from its Little Ice Age (LIA) maximum extent (Lea et al., 2014a). The post-LIA
9 glacial geomorphology of KNS has been mapped, while previous analysis of a
10 photograph taken in the 1850s, and a map published in 1859 places the terminus
11 position somewhere inside the limit of a significant glacier readvance/stillstand (Lea
12 et al., 2014a). We refer to this as the Akullersuaq Stade (after the headland that its
13 maximum extent adjoins), previously referred to as the '1920 Stade' (Weidick et al.,
14 2012). This event is renamed due to the uncertainty of the exact timing of the glacier
15 maximum.

16 Where the full terminus cannot be observed in photographs, terminus position
17 is determined indirectly using the GIS based analyses described below, in
18 conjunction with evidence from maps (e.g. Lea et al., 2014a). Subsequent to 1921,
19 intermittent direct observations of the terminus are available, enabling mapping of
20 terminus positions from imagery (list of sources in Table 1).

21 Landsat panchromatic band imagery was used to map terminus positions for
22 1987-2012. Cloud-free Landsat scenes were selected for analysis, acquired as late
23 in the melt season as possible, or just after its end. The start of November was used
24 as the latest date from which images could be selected, since beyond this, *mélange*
25 in the fjord has been observed to freeze, causing the terminus to advance
26 (Mortensen et al., 2011; Sole et al., 2011). The majority of images were acquired
27 during September or October, though for 1993 and 2003 cloud-free images were
28 only available for dates in August (30 August 1993 and 9 August 2003 respectively).
29 No suitable images were available for the years 1988-1991 and 1998, meaning that
30 annual resolution rates of terminus change were acquired for 1992-1997 and 1999-
31 2012 (Table 1).

32 For the entire length of the record, where more than 1 year separated
33 terminus observations, annually averaged rates of change were calculated. This
34 provides a continuous record of the trends in behaviour, and inter-annual variability

1 of KNS for the period spanning 1859-2012. This behaviour could then be directly
2 compared to atmospheric and oceanic climate data.

3 Each terminus position was quantified using an adaptation of the box method
4 (Moon and Joughin, 2008; Howat and Eddy, 2011), called the Curvilinear Box
5 Method (CBM; see Lea et al., 2014b, for details). This has a marked advantage over
6 the centreline tracking or standard box methods as it is capable of accounting for
7 changes in terminus geometry, while also accurately tracking changes in fjord
8 orientation (Lea et al, 2014b). Furthermore, the box used to calculate terminus
9 change is always centred on the glacier/fjord centreline, which is also the flowline
10 used for the numerical model. Consequently, terminus positions and observed
11 changes in position derived using the CBM can be compared directly to model
12 output.

13

14 **4. The TWG Model**

15 The numerical model used is specifically designed to simulate the dynamics of
16 TWGs along a flowband (Nick et al., 2010). It has been successful in replicating the
17 dynamics of marine terminating outlets in both Greenland (e.g. Vieli and Nick, 2011;
18 Nick et al., 2012; Lea et al., 2014a) and Antarctica (Jamieson et al., 2012; 2014),
19 and has also been used to make centennial timescale projections of the future
20 contribution of Greenland's major TWG outlets to global sea level (Nick et al., 2013).
21 The model uses a stretched grid, allowing a robust treatment of grounding line
22 dynamics (Pattyn et al., 2012), while basal, lateral and longitudinal shear stresses
23 are accounted for. Bed topography data for the majority of the catchment are
24 provided by Bamber et al., (2001), though the lower 40 km is generated using a
25 mass continuity based bed reconstruction (Morlighem et al., 2011), validated against
26 available OIB/CReSIS flightlines (Gogineni et al., 2001). Fjord width (Figure 3c) is
27 defined as the sum of the minimum linear distances from a point on the flowline to
28 either side of the fjord (Figure 3a). Where available, fjord bathymetry data are also
29 used where KNS has retreated following its LIAMax (Figure 3c; Weidick et al., 2012).
30 Sensitivity analyses conducted by Lea et al. (2014a; their Figure 10) for this bed
31 configuration demonstrated that the model exhibits broadly comparable patterns of
32 retreat behaviour where bed elevation is varied within an uncertainty of ± 50 m.

1 A constant height versus SMB relation is used to calculate SMB for the
 2 ablation zone of KNS (Eqn. 1). This is derived from the average RACMO SMB model
 3 output for 1958-2007 (Ettema et al., 2009).

$$4 \quad b(x) = 0.0018 \times h(x) - 2.693 \quad (1)$$

6
 7 Where $b(x)$ is the SMB for position x (the along-flow coordinate) on the model
 8 flowline, and $h(x)$ is the glacier elevation for position x on the flowline. Due to the
 9 tendency for over-estimation of accumulation in RACMO in this region (Van As et al.,
 10 2014), positive SMB values in the upstream section of the modelled glacier are
 11 prescribed to be lower than the RACMO output, allowing the glacier to maintain its
 12 contemporary elevation profile. Irrespective of this, SMB forcing has previously been
 13 demonstrated to be of minimal importance to results of modelled TWG dynamics
 14 over the timescales that are being investigated (Lea et al., 2014a). The model is
 15 initialised using a glacier geometry approximating that of the Akullersuaq Stade
 16 maximum (ASM), derived from geomorphological mapping of associated trimlines
 17 (Figure 1). Constants and parameter values used are summarised in Table 2, while
 18 the initial tuning procedure followed for this configuration is the same as that used by
 19 Lea et al. (2014a). Surface runoff (Van As et al., 2014), air temperature (JJA
 20 average) and SST (annual average) data are used to drive changes in crevasse
 21 water depth (d_w) and submarine melting (M), respectively.

22 Although seasonal cycles in velocity are observed at KNS within 20 km of its
 23 terminus (Ahlstrøm et al., 2013), at locations >35 km from the terminus these have
 24 been demonstrated to have negligible effect (~1%) on net annual motion (Sole et al.,
 25 2011). Given that the timescales of interest are annual to decadal, seasonal
 26 variability in basal and lateral sliding is therefore not included within the model
 27 experiments. The model uses an effective pressure sliding law, allowing it to
 28 replicate a typical tidewater glacier velocity profile, accelerating towards its terminus.
 29 Two zones of constant basal roughness (upstream and downstream) are prescribed
 30 to allow the model to replicate observed elevation and velocity profiles (Lea et al.,
 31 2014a). This also ensures that particular areas of the fjord are not biased towards
 32 advance/retreat behaviour. All parameters which control the model sensitivity to
 33 climate forcing are derived using the Monte Carlo methods described below.

1 **4.1 Relating crevasse water depth to air temperature**

2 Changes in the value of d_w have previously been related to runoff variability (e.g.
 3 Nick et al., 2010; Cook et al., 2012; 2013), and have been successfully used as a
 4 climate-linked forcing directly affecting terminus change (Nick et al., 2013). This is
 5 achieved via a physically based crevasse water depth calving criterion (Benn et al.,
 6 2007), where crevasse penetration depth, and potential for calving, is enhanced by
 7 d_w . However, the only previously used scaling of surface runoff to d_w requires a
 8 baseline d_w value to be prescribed, which it cannot fall below (Nick et al., 2013, their
 9 equation S3). To remove the need to define a minimum d_w value at the beginning of
 10 each model run, we present a new, unrestricted parameterisation that relates
 11 seasonal changes in monthly surface runoff to d_w , and allows d_w to freely evolve due
 12 to changes in annual runoff (Eqn. 2).

13

$$14 \quad d_{wNew} = d_{wPrev} + \alpha_1 \left(R_{year} \beta_{month} - \frac{R_{base}}{12} \right) \quad (2)$$

15

16 Where d_{wNew} is the new crevasse water depth for a particular month, d_{wPrev} is the
 17 crevasse water depth from the previous month, α_1 is the coefficient relating crevasse
 18 water depth sensitivity to changes in runoff, R_{year} represents total runoff for a given
 19 year (Gt yr^{-1}), β_{month} is the fraction of annual runoff occurring in a particular month,
 20 R_{base} is a baseline/long term average annual runoff total (Gt yr^{-1}), equivalent to the
 21 annual volume of water that is either refrozen within the glacier or drains from the
 22 crevasse to the bed. This assumes that the rate of refreezing/drainage of water from
 23 crevasses is constant from year to year. Where annual runoff exceeds R_{base} , the
 24 average annual d_w will therefore increase, and where runoff falls below R_{base} , the
 25 average annual d_w will decrease. Dividing annual runoff into each month's
 26 contribution also allows the direct incorporation of d_w 's seasonal variability. The
 27 value of d_w will therefore reach its annual minimum prior to the onset of the melt
 28 season, and peak in August. The coefficient α_1 allows the sensitivity of d_w to changes
 29 in runoff to be adjusted, and is used as a tuning parameter.

30

31 **4.2 Definition of β_{month}**

32 The fraction of annual runoff occurring in each month, β_{month} , is derived from analysis
 33 of each month's average runoff from the catchments of both KNS and Akullersuaq

1 Sermia (AS) over the period 1960-2012, as given by high resolution surface mass
 2 balance (SMB) modelling of the region (Van As et al., 2014). The runoff values for
 3 KNS and AS are summed since the glaciers were confluent for much of the time
 4 since their LIAMax, including a significant portion of the period of interest of this
 5 study (see below, and Wedick et al., 2012). Monthly runoff estimates were generated
 6 using both Modèle Atmosphérique Régional (MARv3.2; Fettweis et al., 2011), and
 7 the Regional Atmospheric Climate Model (RACMO2; Van Angelen et al., 2013). The
 8 variability in the monthly fraction of annual runoff for the period 1960-2012 is shown
 9 for both models in Figure 2, with each producing similar patterns and magnitudes of
 10 monthly variability. We took the median result from the monthly averages of the two
 11 models. This pattern of monthly variability was kept constant from year to year for
 12 each model run.

13 While the model can be forced directly with annual modelled runoff values for
 14 the period 1960-2012 (Van As et al., 2014), no such values are available for the
 15 century before. Runoff values prior to 1960 are therefore estimated using the relation
 16 that exists between average June, July, August (JJA) air temperatures (A_{JJA}) from
 17 Nuuk for 1960-2012 (Cappelen et al., 2012) and the modelled runoff values ($r =$
 18 0.75). A regression equation is generated from this (Eqn. 3), allowing runoff
 19 estimates ($Gt\ a^{-1}$) for the period 1866-1959 to be made from the Nuuk air
 20 temperature ($^{\circ}C$) record (Vinther et al., 2006; Cappelen et al., 2012).

21

$$22 \quad R_{year} = 0.91 \times A_{JJA} - 1.53 \quad (3)$$

23

24 Combined with the 1960-2012 modelled values, this produces a continuous record
 25 of estimated annual runoff for 1871-2012. Average monthly variability in runoff is
 26 superimposed on this record using the β_{month} term.

27

28 **4.3 Confluence with AS: adjustments to d_w and ice flux**

29 While KNS and AS are confluent in model simulations, variability in d_w at the
 30 terminus is driven by total runoff values from both catchments. The confluence area
 31 of the two glaciers is defined on the model flowline as being 5 km across, lying
 32 between 4 km and 9 km from the 2012 terminus position. However, as KNS retreats
 33 through the confluence with AS the runoff contribution from AS to the terminus is
 34 removed, meaning that d_w needs to be scaled to reflect this. Modelled annual runoff

1 totals for each catchment show that KNS and AS respond directly in phase with one
 2 another ($r = 0.99$), with KNS accounting for 70.3% (MARv3.2) or 74.6% (RACMO2)
 3 of total runoff (Van As et al., 2014). To allow for this reduction in runoff as KNS
 4 retreats through the confluence, the value of d_w is multiplied by a scale factor, γ , that
 5 will have a fixed value for each model run of between, α_2 (a confluence scaling
 6 factor) and 1, such that

$$8 \quad d_{wNew} = \gamma d_{wPrev} \quad (4)$$

9
 10 Because AS and KNS will at times be partially confluent, the value of γ is also scaled
 11 linearly with respect to the relative position of the terminus through the confluence,
 12 such that when they are fully confluent $\gamma = 1$, and when fully diffluent $\gamma = \alpha_2$. Values
 13 are varied linearly between α_2 and 1 for terminus positions within the confluence
 14 according to

$$16 \quad \gamma = \alpha_2 + (1 - \alpha_2) \left(\frac{x_{conf}}{X_{conf}} \right) \quad (5)$$

17
 18 Where x_{conf} is the distance of the terminus through the confluence, and X_{conf} is the
 19 total flowline distance over which the confluence occurs. Due to uncertainty
 20 regarding the precise scaling of runoff to d_w as KNS retreats through its confluence
 21 with AS, and other confluence effects, α_2 is used as a tuning parameter within the
 22 model.

23 The extra ice flux contribution from AS when confluent with KNS is estimated
 24 to be approximately one sixth of that of KNS, based on the contemporary across
 25 glacier velocity profiles (Joughin et al., 2010), and terminus widths of AS and KNS.
 26 This extra flux is added to the modelled glacier as positive SMB at the confluence of
 27 KNS and AS, distributed along the flowline proportionate to the contemporary AS
 28 across glacier velocity profile (Lea et al., 2014a).

29

30 **4.4 Relating submarine melt to sea surface temperature**

31 Submarine melt rate (M) has previously been linearly related to deep ocean
 32 temperature (DOT) variability using a scaling coefficient (Nick et al., 2013; their
 33 equation S2). Using this parameterisation, the highest values of M (expressed in this

1 study in $\text{km}^3 \text{a}^{-1}$) are associated with the highest scaling coefficients. Therefore high
 2 scaling factor values would also be linked to the highest inter-annual variability of M .
 3 This study takes a slightly different approach in that (1) M is scaled to sea surface
 4 temperature (SST) rather than DOT, for reasons relating to fjord circulation explained
 5 above, and (2) we introduce a constant (minimum) baseline M rate, M_{base} , which is
 6 added to the linear relation with SST. We therefore calculate M ($\text{km}^3 \text{a}^{-1}$) according to

$$8 \quad M = M_{base} + \alpha_3 T_{year} \quad (6)$$

9
 10 Where α_3 is a submarine melt rate scaling coefficient, and T_{year} is the annual average
 11 SST. This allows multiple minimum background rates M_{base} to be tested for different
 12 model runs, with various sensitivities of M to changes in SST superimposed upon
 13 this using α_3 .

14

15 **4.5 Model experiments and evaluation**

16 Tuning parameters α_1 , α_2 , α_3 and M_{base} were varied randomly within prescribed limits
 17 for a total of 1500 Monte Carlo style model runs. These were defined at the start of
 18 each run's spin up period and held constant throughout. The limits for each of the
 19 tuning parameters were: (1) α_1 , between 0 and 1.5, (2) α_2 , between 0.3 to 0.8, (3)
 20 M_{base} , between 0 to $0.7 \text{ km}^3 \text{a}^{-1}$, and (4) α_3 , between 0 to 0.3. These ranges of α_1 and
 21 α_2 were chosen to reflect a wide range of potential forcing scenarios, while the
 22 values of M_{base} and α_3 were chosen so total submarine melt rates could potentially
 23 range from $0 \text{ km}^3 \text{a}^{-1}$ to values that exceed those estimated for other TWGs in
 24 western Greenland (Rignot et al., 2010; Enderlin and Howat, 2013). This allowed the
 25 different potential drivers of the observed terminus change to be comprehensively
 26 assessed. Runs were conducted for the period 1871-2012, given that this is the
 27 period that both atmospheric and oceanic climate records are available for. The
 28 model was initialised at approximately the ASM profile and terminus position, as
 29 defined by the geomorphology, and given the duration of the spin up period to
 30 stabilise for the given forcing scenario. During spin up, d_w was allowed to freely
 31 evolve by up to $\pm 3 \text{ m a}^{-1}$ to allow the terminus to stabilise at the ASM, with R_{base} and
 32 T_{year} held constant. These were defined as the 1871-1920 runoff average (3.107 Gt

1 yr⁻¹) and SST average (2.605 °C) respectively. These values were used for spin up
 2 as it is known the ASM was attained at some point within this time window.

3 Model results were evaluated against their ability to replicate observed
 4 terminus dynamics, where absolute terminus positions are known (i.e. 1921 to 2012).
 5 The period from 1871-1920 therefore effectively becomes a transient spin up period,
 6 where the model is driven using real climate data though terminus position is only
 7 known within a range. The ability of each model run to replicate observed dynamics
 8 was determined using a weighted regression (R^2) calculation, with the weighting of
 9 each terminus observation calculated according to

10

$$11 \quad w_n = \frac{D_{n+1} - D_{n-1}}{2(D_k - D_1)} \quad \text{for } n = 1, 2, \dots, k \quad (7)$$

12

13 Where w is the observation weighting in the regression calculation, n is the terminus
 14 observation, k is the total number of terminus observations, and D is the date of the
 15 terminus observation. Each terminus observation is therefore temporally weighted
 16 according to the median length of time elapsed between the terminus observations
 17 that occur before and after observation n . This ensures that the evaluation of model
 18 performance is not biased towards the last ~20 years where there is a comparatively
 19 high density of observations. Model runs were counted as successful where (1) the
 20 difference between the modelled and observed 1921 position was <500 m, (2) the
 21 weighted $R^2 > 0.85$, and (3) the gradient of the resulting line of regression was >
 22 0.85.

23

24 **5. Glacier reconstruction results**

25 The geomorphology shows distinct upper and lower sets of lateral moraines on both
 26 sides of the fjord, with fluted moraines occupying the intervening space (Figure 1a).
 27 The upper set are associated with the LIA maximum (Lea et al, 2014a), while the
 28 lower set were formed during the Akullersuaq Stade. Fridtjof Nansen's (1890)
 29 account of the first traverse of Greenland in 1888, includes a drawing from a
 30 photograph showing AS and KNS to be confluent, though the terminus position itself
 31 is not visible. Although the original image could not be traced or an exact date of
 32 acquisition determined, it is likely to have been taken some time near to the
 33 publication date of 1890.

1 Maps from 1859, 1860, 1866 and 1885 all show the terminus of KNS to be
2 adjoining Akullersuaq and fully confluent with AS (Kleinschmidt, 1859; Poulsen,
3 1860; Brede, 1866; Rink, 1866; Jensen, 1885). While it is possible that some details
4 on the maps were copied following Kleischmidt (1859), the addition of detail such as
5 lakes on plateaus near to KNS by Jensen (1885) provides confidence that this map
6 faithfully records the contemporary terminus position. There is nothing to suggest
7 that KNS became diffluent from AS at any time from 1859-1885. However, due to a
8 lack of map detail and the Nansen (1890) drawing not including the terminus, these
9 sources cannot be used to provide absolute terminus positions.

10 The earliest images of KNS are from the 1850s and 1903. Both are taken
11 from approximately the same position, with the terminus partially obscured by
12 foreground topography (Weidick et al., 2012). The presence of medial moraines in
13 each image demonstrates that KNS was confluent with AS. Lea et al., (2014a)
14 quantified the terminus position uncertainty for the 1850s photograph using viewshed
15 analysis. Similar analysis has been undertaken for the 1903 image, showing that the
16 uncertainty in terminus position is the same as for the 1850s image (Figure 3). The
17 maximum terminus extents for both images are therefore located behind a headland
18 corresponding to the ASM on the eastern side of the fjord (Figures 1a, 3).

19 It is not currently possible to say from any observational evidence when the
20 ASM was attained, only that it occurred sometime between 1859-1920. The climate
21 anomalies for the period (compared to 1961-1990 baselines) show that air
22 temperature (AT) and SST anomalies were, on average, antiphased for the period
23 1871-1903 (Figures 4c, d), though AT and SST anomalies are in phase
24 (negative/near-baseline) for 1903-1920. Conditions are therefore more likely to have
25 been conducive for glacier advance during the latter period.

26 Terminus position was mapped directly for the remaining images, providing a
27 record of 29 terminus positions spanning the period 1921-2012 (Figures 1 and 4).
28 The first direct terminus observation (1921) shows a slight retreat from the ASM.
29 Subsequent to this, KNS retreated a total of 9.7 km at a non-uniform rate up to 2012,
30 interrupted by short periods of readvance (Figures 4a, b). Averaged retreat rates of -
31 116 m a^{-1} are observed between 1921-1946, before a rapid retreat of 3.9 km within
32 the 2 year period from 1946-1948 (Figures 1a, 4). Between 1948-1968 KNS
33 retreated on average by -97 m a^{-1} , before readvancing by $+60 \text{ m a}^{-1}$ up to 1979

1 (Figure 4b). A terrestrial photograph taken in 1965 with the majority of the terminus
2 obscured shows the termini of KNS and AS to be fully diffluent.

3 The 1921-1968 period of sustained retreat was accompanied by positive
4 average AT and SST anomalies (Figures 4c, d). The highest AT anomalies occurred
5 during the period 1928-1941, though the largest retreat (between 1946-1948)
6 occurred during a comparatively less extreme period of positive AT and SST (Figure
7 4).

8 From 1979 to 1987 KNS retreated by -658 m in total (-82 m a^{-1}), before
9 readvancing by +758 m from 1987-1992 ($+152 \text{ m a}^{-1}$). Using the near complete 20
10 year annual record of terminus fluctuations from 1992-2012, KNS advanced for 4 out
11 of 5 years between 1992-1997, followed by retreat in 11 out of 13 years from 1999-
12 2012 at an average rate of -103 m a^{-1} . The latter included 8 annual retreats of >100
13 m, with the largest retreats occurring in 2004 (-438 m) and 2005 (-316 m). These
14 periods of advance and retreat behaviour occurred during periods of in-phase
15 negative and positive climate anomalies respectively.

16 Where temporal density of observations was high, terminus behaviour that
17 was antiphased with the prevailing climate anomalies was also observed (i.e.
18 advancing during positive temperature anomalies, or retreating during negative
19 temperature anomalies). Examples of this include a retreat of -626 m in 1995 when
20 both climate anomalies were negative, while terminus advances occur in 2008 and
21 2009 despite markedly positive AT and SST anomalies (Figure 4). At annual
22 resolution, the magnitude of terminus retreat/advance was also found to be unrelated
23 to the magnitude of either climate anomaly for each particular year.

24 Based on interpolated terminus positions between observations, terminus
25 widths were consistent at ~ 3.5 km from 1932-1946, and ~ 4.2 km from 1968-2012
26 where terminus change was comparatively slow (Figure 5b). Although fjord depths at
27 the terminus for these periods were more variable, they did not exceed a range of
28 ± 22 m. Fjord width and depth at the terminus displayed two step changes during the
29 retreats between 1921-1932, and 1946-1948 (black lines, Figures 5a-c). During the
30 first of these, both width and depth increased (by ~ 550 m and 44 m respectively)
31 whereas during the second, width increased but depth decreased (by ~ 700 m and
32 146 m respectively).

33

34 **6. Model results**

1 From a total of 1500 model runs conducted, 29 runs (1.9%) successfully replicated
2 the observed dynamics of KNS according to the criteria outlined above (Figure 5).
3 Following the initiation of climate forcing in 1871 (Figures 5d, 5e), the results of each
4 run are highly comparable up to 1884, with little modelled terminus change
5 observed. Following this, for the period 1884 to ~1910, 6 of the 29 runs (21%) show
6 evidence of multi-annual terminus retreats and equivalent readvances of >750 m
7 with periodicities of 2-4 years. A further 7 runs (24%) show evidence of at least one
8 short lived (<5 year) oscillation in terminus position of >750 m between 1884 to
9 1920. None of these model runs significantly exceed the ASM position, and are thus
10 in agreement with the geomorphological evidence presented, and the position of the
11 1921 terminus observation.

12 All model runs retreat to the observed 1932 position between modelled years
13 1929-1936, via a single retreat event of ~1 km. Subsequent to this, modelled retreat
14 to the observed 1946 position is gradual, before the model successfully replicates a
15 large topographically controlled retreat from the 1946 position. There was varying
16 success in modelling the exact timing of this retreat (observed between 1946-1948),
17 with the model ensemble predicting it to occur anywhere between 1943-1962. The
18 position where the modelled terminus restabilises following the retreat through the
19 AS confluence is generally too far advanced by ~1 km compared to the position
20 following the 1946-1948 retreat. All model runs then go on to over-predict terminus
21 extent for the 1968 observation by between 0.35 to 1.59 km.

22 Though no model runs exactly match the precise inter-annual terminus
23 fluctuations from 1968-2012, they do capture the general multi-annual to decadal
24 pattern of retreat observed. This is characterised by general terminus stability within
25 a range of ± 500 m for the period 1968 to ~1999, before the terminus begins to
26 retreat ~2 km towards the 2012 position. All of the successful model runs identified
27 predict KNS to be in a more retreated position in 2012 than observed by a range of
28 0.32 to 5.04 km.

29 Where a significant difference between observed and modelled terminus
30 positions has occurred by the end of the model run in 2012, the divergence begins in
31 2010 at the earliest. This coincides with a widening of the modelled fjord associated
32 with the uncertainty in fjord topography upstream of the contemporary terminus
33 (Figure 5b).

1 The distributions of tuning parameters for successful runs are shown in Figure
2 6, with the distribution of all histograms shown to be non-normal. Submarine melting
3 related tuning parameters, α_3 , and M_{base} , tended towards the mid to lower ends of
4 the ranges tested (Figures 6c, 6d). Values of α_3 peak between 0.075 to 0.1, though
5 there is no clearly defined peak in the distribution of M_{base} values.

6 In contrast, none of the d_w related tuning parameters (α_1 and α_2) approach 0
7 (Figures 6a, 6b), with the lowest values being 0.412 and 0.389 respectively.
8 Construction of a correlation matrix comparing all tuning parameter values for all
9 successful runs also demonstrates a significant inverse relationship between the
10 value of α_1 , and the AS confluence parameter, α_2 ($r = -0.92$). While other significant
11 correlations are observed (Table 3), these are not of sufficient strength to allow
12 confident conclusions to be drawn.

14 **7. Discussion**

16 **7.1 Observed terminus behaviour**

17 From 1903 to 2012 AT and SST anomalies covaried, with the terminus generally
18 undergoing retreat during periods of positive anomalies and advancing/stabilising
19 when near/below baseline climate (Figure 4). Exceptions to this in-phase behaviour
20 were only identified for the period 1992-2012, where a higher temporal density of
21 terminus observations exists. However, by averaging annual observations over
22 periods of sustained negative (1987-1997) and positive (1998-2012) climate
23 anomalies, the terminus responds in phase with the climate anomalies. This
24 demonstrates the risks of using short datasets (2-5 years) to determine how a TWG
25 is responding to climate forcing, highlighting the inherent noisiness, potential
26 importance of antecedence, and the non-linearity of TWG response to climate.

27 A notable caveat to this occurs where significant topographically controlled
28 glacier retreats occur (i.e. those driven by changes in fjord width and/or depth).
29 These events could potentially skew annually averaged terminus change rates when
30 attempting to characterise terminus response to climate forcing. The relative
31 importance of this will be entirely dependent on the magnitude of individual events,
32 and most significant where there is potential for multi-kilometre topographically
33 controlled retreat. For example, if the 1946-1948 retreat event was not temporally

1 well constrained, it could have significantly biased the terminus change rate values
2 between 1936-1968 (Figure 4b).

3 The 1946-1948 retreat occurs where the fjord widens and shallows at the
4 terminus, while the 1921-1932 retreat is associated with a fjord widening and
5 deepening (Figures 5a-c). The 1946-1948 retreat is therefore likely to have been
6 controlled by changes in lateral topography rather than basal topography, whereas
7 the 1921-1932 retreat (if it occurred rapidly, e.g. in 1-2 years) likely resulted from a
8 combination of both. In the periods between these >1 km retreats, both fjord width
9 and depth at the terminus remained largely consistent (Figures 5b,c). While
10 kilometre scale, rapid retreat of KNS is likely due to a combination of retreat into fjord
11 widenings or deepenings (e.g. Mercer, 1961; Carr et al., 2013; 2014; Porter et al.,
12 2014) the 1946-1948 retreat helps to demonstrate that destabilising changes in one
13 aspect of fjord topography can dominate stabilising changes in the other, until a new
14 equilibrium is reached.

15 Since TWGs exhibit varying degrees of non-linearity in response to climate
16 forcing, the identification of where and when these rapid multi-kilometre retreat
17 events occur is crucial for interpreting the causes of terminus fluctuations. Where
18 comparatively smaller (i.e. <500 m) climatically anti-phased advance/retreat events
19 occur, their effect on average terminus change rates can be mitigated by averaging
20 change over timescales up to, or greater than a decade. For example, extending the
21 1992-1997 average (51 m a⁻¹ retreat) to cover the period 1987-1997 (91 m a⁻¹
22 advance) provides a more representative impression of multi-annual terminus
23 behaviour, since 5 out of the 6 observations available show terminus advance.
24 Where observations are separated by >1 year, interpreting the absolute values of
25 terminus change rates should therefore be done with caution. In most cases these
26 values will be more representative of the average direction (i.e. advance/retreat),
27 rather than the average distance of terminus change.

28 Taking into account uncertainties due to topographic controls on terminus
29 stability, observations of terminus change over a period of several years provide a
30 better indication of a TWG's response to climate forcing. However, for this study,
31 deconvolving the relative importance of AT versus SST in driving terminus change is
32 difficult using observations alone, given that both climate drivers vary in phase for
33 1903-present. It could potentially be argued that AT is the primary driver of change,
34 since the 33 year period of positive anomaly SST from 1871-1903 had relatively little

1 impact on the terminus stability of KNS. However, a narrow, and relatively shallow
2 fjord geometry in this region could also have been a significant factor in stabilising
3 the terminus during this time (Figure 3c). Arguably this becomes less likely when it is
4 considered that while SST was similar for the period 1921-1948, positive AT allowed
5 KNS to retreat through the same section of fjord and through its confluence with AS
6 within 26 ± 1 years (Figure 4). However, given the lack of certainty in terminus
7 position between 1871-1920, it is not possible to robustly verify these arguments.

8

9 **7.2 Implications of modelling**

10 The observed terminus behaviour of KNS from 1921-2012 was successfully
11 replicated by 29 of 1500 model runs using surface runoff and SST records as drivers
12 of terminus change. This demonstrates that the parameterisations used to scale
13 these climate records to d_w and M respectively can successfully be used to simulate
14 the observed pattern of tidewater glacier behaviour over centennial timescales.
15 Where the observational record is of sufficient detail to resolve inter-annual terminus
16 fluctuations (1992-2012), the model does not replicate these. This is to be expected
17 given (1) the flowband nature of the model and associated depth and width
18 integrations over each grid cell, meaning that fluctuations of terminus configurations
19 such as the creation of calving bays cannot be replicated (e.g. Figure 1b), (2) the
20 uncertainty in fjord bathymetry and geometry potentially affecting relative terminus
21 stability, and (3) the use of single terminus observations as notionally definitive
22 indicators of annual terminus change, where the stochastic nature of calving and
23 associated sub-annual terminus fluctuations make any direct one-to-one
24 comparisons to modelled results inappropriate. Valid comparison of model results to
25 observations should therefore only be attempted over multi-annual timescales where
26 terminus dynamics within calving bays, sub-annual calving events and fine scale
27 uncertainties in fjord, and basal topography become comparatively less significant.

28 For successful model runs, the interrelationships between the parameter
29 values that determine d_w and M sensitivity to the climate records also inform the
30 relative importance of changes in atmospheric and oceanic forcing in driving
31 terminus change. The lack of any significant relationship between α_1 and α_3
32 demonstrates that a change in model sensitivity to surface runoff is not offset by any
33 change in model sensitivity to SST (e.g. a higher α_1 would not need to be offset by a
34 lower α_3 for the model run to match observations). Taken alone, this evidence

1 indicates that either atmospheric forcing (via surface runoff) dominates oceanic
2 forcing (via SST), or *vice versa*. However, the occurrence of runs where α_3 does not
3 significantly exceed 0 (i.e. where runs experience negligible M variability)
4 demonstrate that the model can successfully reproduce observed behaviour with
5 nearly no changes in oceanic forcing from year to year. Although some successful
6 model runs did have significant inter-annual M variability (e.g. the maximum range of
7 M values for an entire 141 year model run was $0.76 \text{ km}^3 \text{ a}^{-1}$), each model run always
8 requires significant atmospheric forcing variability to allow it to replicate
9 observations. The importance of oceanic forcing variability can therefore not be
10 entirely discounted.

11 The model demonstrates that knowledge of atmospheric forcing (via runoff),
12 without needing to vary oceanic forcing, can be sufficient to reproduce realistic
13 patterns of observed glacier behaviour at KNS over the last century. However, the
14 precise physical mechanism by which air temperature could drive observed change
15 requires further investigation. For example, though a combination of modelled and
16 empirically estimated runoff values have been used to drive changes in d_w to force
17 the model, subglacial runoff variability is also known to drive rates of submarine
18 melting at the terminus (Jenkins, 2011; Xu et al., 2012; Sciascia et al., 2013).
19 Therefore we do not rule out that the behaviour observed could also be explained by
20 calving driven by seasonal changes in submarine melt rates, that are in turn a
21 function of subglacial runoff (e.g. Sciascia et al. 2013).

22 The relative insensitivity to changes in oceanic forcing is not necessarily
23 surprising given the hydrographic setting of KNS – located at the end of a >100 km
24 long fjord system that is thought to be largely insulated from changes in ocean
25 conditions due to the presence of a shallow sill at its entrance (Mortensen et al.,
26 2011; 2013). This has previously been used to suggest that recent changes in ocean
27 conditions (e.g. Straneo and Heimbach, 2013) have not affected the dynamics of
28 KNS significantly (Straneo et al., 2012). The results presented here are therefore
29 compatible with this argument.

30 The over-estimation of terminus retreat by 2012 of every successful run is
31 thought to result from the poor knowledge of fjord width geometry beyond the
32 contemporary glacier terminus. Upstream of the 2012 terminus, the lateral ice
33 margins are used to define model glacier width, leading to a likely over-estimation of
34 the prescribed fjord width. The divergence between the actual and prescribed fjord

1 width is likely to increase upglacier, increasing the likelihood of model error in this
2 area. This explains why significant divergence from the observational record only
3 occurs once the modelled terminus has retreated ~1.5 km beyond the 2012 terminus
4 (Figures 5a-c). Given the shallowing of the fjord bathymetry upstream of the 2012
5 terminus (Figure 5c), fjord width uncertainty is likely to be the major cause of the
6 model over-estimating retreat (Figure 5b). This also substantiates observations that
7 destabilising changes in fjord width can dominate stabilising changes in fjord depth.
8 Any attempt at modelling the future fluctuations of KNS will therefore require both
9 improvements to subglacial topography estimates and comprehensive assessments
10 of fjord width uncertainties as part of any predictions.

11

12 **8. Conclusions**

13 Utilising multiple lines of evidence, it has been possible to reconstruct terminus
14 fluctuations of KNS from 1859-2012. This study therefore completes the record of
15 terminus fluctuations of KNS from its LIAMax, in 1761 (Lea et al., 2014a), up to the
16 present, providing one of the longest, and most detailed records of observed TWG
17 change in Greenland. The length and detail of this record, in conjunction with
18 existing datasets providing boundary conditions, therefore make KNS an ideal
19 validation site for models aiming to simulate outlet glacier retreat, and/or the impact
20 of calving on tidewater glacier dynamics. At present the major boundary condition
21 uncertainty is fjord topography, though what is known is sufficient for the model used
22 in this study to replicate observed dynamics over multi-decadal to centennial
23 timescales.

24 Results from numerical modelling show that the fluctuations of KNS can be
25 simulated through parameterisations that link surface runoff to a crevasse water
26 depth based calving criterion. Changes in crevasse water depth and/or runoff driven
27 rates of submarine melt are therefore suggested as potential drivers of observed
28 change. Although ocean driven changes in submarine melt rates are not always
29 required for the model to replicate the observed length variations of KNS, results do
30 not allow their importance to be discounted entirely.

31 Observations of KNS show it to respond in phase with AT and SST anomalies
32 over multi-annual to decadal timescales from at least 1921-2012 (i.e. retreating
33 during positive temperature anomalies, and advancing during negative temperature
34 anomalies). However, where inter-annual comparisons to AT and SST are possible

1 (1992-2012), climatically anti-phased terminus fluctuations are observed. This
2 highlights the inherent noisiness of terminus response over short timescales, the
3 potential importance of antecedence, and the dangers of using similarly short
4 calibration periods for predictive modelling efforts.

5 Results from numerical modelling successfully capture the terminus dynamics
6 of KNS over multi-annual to decadal timescales, though not precise inter-annual
7 fluctuations. This is due to a combination of uncertainties in fjord topography, and the
8 approximations inherent to the depth and width integrations associated with using a
9 one-dimensional flow-band model.

10 Nevertheless, this study demonstrates that simple flow-band numerical
11 models of tidewater glaciers can be used to capture TWG dynamics over multi-
12 annual to centennial timescales. This provides validation that these models can be
13 useful tools for palaeo, contemporary, and prognostic modelling efforts. However,
14 the primary challenge to their use as predictive tools remains the accurate definition
15 of subglacial topography and fjord width, which exert dominant controls on glacier
16 stability. Any future efforts at prognostic modelling of TWGs should therefore seek to
17 account for these uncertainties in addition to those associated with sensitivity to
18 climate forcing.

19

20 **Acknowledgements**

21 The authors wish to thank Stephen Price, Mauri Pelto and an anonymous reviewer
22 for their reviews and comments that helped to improve the manuscript. RACMO2.1
23 data were provided by Jan van Angelen and Michiel van den Broeke, IMAU, Utrecht
24 University. MAR v3.2 data used for runoff calculations were provided by Xavier
25 Fettweis, Department of Geography, University of Liège. The photogrammetric DEM
26 used in Figures 1 and 3 was provided by Kurt H. Kjær, Centre for GeoGenetics,
27 University of Copenhagen. This research was financially supported by J.L.'s PhD
28 funding, NERC grant number: NE/I528742/1. Support for F.M.N. was provided by the
29 Conoco-Phillips/Lundin Northern Area Program CRIOS project (Calving Rates and
30 Impact on Sea Level).

31

32 **References**

33 Alley, R. B., Andrews, J. T., Brigham-Grette, J., Clarke, G. K. C., Cuffey, K. M.,
34 Fitzpatrick, J. J., and 7 others: History of the Greenland Ice Sheet: paleoclimatic

- 1 insights. *Quaternary Science Reviews*, 29(15), 1728-1756, 2010. DOI:
2 10.1016/j.quascirev.2010.02.007
3
- 4 Bamber, J. L., Layberry, R. L., Gogineni, S. P.: A new ice thickness and bed data set
5 for the Greenland ice sheet: 1. Measurement, data reduction, and errors. *Journal of*
6 *Geophysical Research: Atmospheres (1984–2012)*, 106(D24), 33773-33780, 2001.
7 DOI: 10.1029/2001JD900054
8
- 9 Bevan, S. L., Luckman, A. J., and Murray, T.: Glacier dynamics over the last quarter
10 of a century at Helheim, Kangerdlugssuaq and 14 other major Greenland outlet
11 glaciers, *The Cryosphere*, 6, 923-937. DOI:10.5194/tc-6-923-2012, 2012.
12
- 13 Brede, N.: *Skizze Kaart over Vestkysten af Grönland fra Arsuk til Holsteensborg*.
14 KBK Netpublikation DK003200, Copenhagen, 1866.
15
- 16 Bjørk, A. A., Kjær, K. H., Korsgaard, N. J., Khan, S. A., Kjeldsen, K. K., Andresen, C.
17 S., Larsen, N.K., Funder, S.: An aerial view of 80 years of climate-related glacier
18 fluctuations in southeast Greenland. *Nature Geoscience*, 5(6), 427-432, 2012. DOI:
19 10.1038/ngeo1481
20
- 21 Bruun, D.: Oversigt over Norburuiner i Godthaab og Frederikshaab Distrikter.
22 *Medelelser om Grønland*. 56(3), 55-147, 1917.
23
- 24 Cappelen, J.: Greenland-DMI Historical Climate Data Collection 1873-
25 2011. *Technical Report 12-04*. Copenhagen, 2012. ISSN: 1399-1388
26
- 27 Colgan, W., Pfeffer, W. T., Rajaram, H., Abdalati, W.: Monte Carlo ice flow modeling
28 projects a new stable configuration for Columbia Glacier, Alaska, by c.
29 2020. *Cryosphere*, 6(2), 893-930, 2012. DOI: 10.5194/tcd-6-893-2012
30
- 31 Cook, S., Zwinger, T., Rutt, I. C., O'Neel, S., Murray, T.: Testing the effect of water in
32 crevasses on a physically based calving model. *Annals of Glaciology*, 53(60), 90-96,
33 2012. DOI: 10.3189/2012AoG60A107
34

- 1 Cook, S., Rutt, I. C., Murray, T., Luckman, A., Selmes, N., Goldsack, A., Zwinger, T.:
2 Modelling environmental influences on calving at Helheim Glacier, East
3 Greenland. *Cryosphere Discussions*, 7(5), 2013. DOI: 10.5194/tcd-7-4407-2013
4
- 5 Csatho, B., Schenk, T., Van der Veen, C. J., Krabill, W. B.: Intermittent thinning of
6 Jakobshavn Isbræ, West Greenland, since the Little Ice Age. *Journal of*
7 *Glaciology*, 54(184), 131-144, 2008. DOI: 10.3189/002214308784409035
8
- 9 Rink, H.: *Kyststrækning fra Frederikshåb i syd til Napasaq i nord*. KBK Netpublikation
10 RI000029, Copenhagen, 1866.
11
- 12 Fettweis, X., Tedesco, M., Broeke, M., Ettema, J.: Melting trends over the Greenland
13 ice sheet (1958–2009) from spaceborne microwave data and regional climate
14 models. *The Cryosphere*, 5(2), 359-375, 2011. DOI: 10.5194/tc-5-359-2011
15
- 16 Gogineni, S., Tammana, D., Braaten, D., Leuschen, C., Akins, T., Legarsky, J. and 4
17 others, K.: Coherent radar ice thickness measurements over the Greenland ice
18 sheet. *Journal of Geophysical Research: Atmospheres (1984–2012)*, 106(D24),
19 33761-33772, 2001. DOI: 10.1029/2001JD900183
20
- 21 Hanna, E., Cappelen, J., Fettweis, X., Huybrechts, P., Luckman, A., Ribergaard, M.
22 H.: Hydrologic response of the Greenland ice sheet: the role of oceanographic
23 warming. *Hydrological Processes*, 23(1), 7-30, 2009. DOI: 10.1002/hyp.7090
24
- 25 Howat, I. M., Eddy, A.: Multi-decadal retreat of Greenland's marine-terminating
26 glaciers. *Journal of Glaciology*, 57(203), 389-396, 2011. DOI:
27 10.3189/002214311796905631
28
- 29 Hvidegaard, S.M., Sorensen, L.S., Forsberg, R.: ASTER GDEM validation using
30 LiDAR data over coastal regions of Greenland. *Remote Sensing Letters*, 3(1), 85–
31 91, 2012. DOI: 10.1080/01431161.2010.527389
32
33

- 1 Jamieson, S. S., Vieli, A., Livingstone, S. J., Cofaigh, C. Ó., Stokes, C., Hillenbrand,
2 C. D., Dowdeswell, J. A.: Ice-stream stability on a reverse bed slope. *Nature*
3 *Geoscience*, 5(11), 799-802, 2012. DOI: 10.1038/ngeo1600
4
- 5 Jamieson, S. S. R., A. Vieli, C. Ó Cofaigh, C. R. Stokes, S. J. Livingstone, and C.-D.
6 Hillenbrand: Understanding controls on rapid ice-stream retreat during the last
7 deglaciation of Marguerite Bay, Antarctica, using a numerical model, *Journal of*
8 *Geophysical Research: Earth Surface*, 119, 247–263, 2014.
9 DOI:10.1002/2013JF002934.
10
- 11 Jenkins, A.: Convection-Driven Melting near the Grounding Lines of Ice Shelves and
12 Tidewater Glaciers. *Journal of Physical Oceanography*, 41(12), 2011. DOI: .
13
- 14 Jensen, J.A.D.: *Vestkysten af Grønland fra Arsuk til Holstensborg 61° til 67° N*. KBK
15 Netpublikation, DK003198. Copenhagen, 1885
16
- 17 Joughin, I., Smith, B. E., Howat, I. M., Scambos, T., Moon, T.: Greenland flow
18 variability from ice-sheet-wide velocity mapping. *Journal of Glaciology*, 56(197), 415-
19 430, 2010. DOI: 10.3189/002214310792447734
20
- 21 Kleinschmidt, S.: *Godthåbs distrikt (hertil en Navneliste)*. (Map No. KBK
22 Netpublikation RI000074). Copenhagen, 1859.
23
- 24 Lea J.M., Mair, D.W.F., Nick, F.M., Rea., B.R., Weidick, A., Kjær, K., Morlighem, M.,
25 van As, D., Schofield, J.E.: Terminus-driven retreat of a major southwest Greenland
26 tidewater glacier during the early 19th century: insights from glacier reconstructions
27 and numerical modelling. *Journal of Glaciology*, 220(60), 2014a. DOI:
28 10.3189/2014JoG13J163
29
- 30 Lea J.M., Mair, D.W.F., Rea, B.R.: Evaluation of existing and new methods of
31 tracking glacier terminus change. *Journal of Glaciology*, 220(60), 2014b. DOI:
32 10.3189/2014JoG13J061
33

- 1 Morlighem, M., Rignot, E., Seroussi, H., Larour, E., Ben Dhia, H., Aubry, D.: A mass
2 conservation approach for mapping glacier ice thickness. *Geophysical Research*
3 *Letters*, 38(19), 2011. DOI: 10.1029/2011GL048659
4
- 5 McFadden, E. M., Howat, I. M., Joughin, I., Smith, B. E., & Ahn, Y.: Changes in the
6 dynamics of marine terminating outlet glaciers in west Greenland (2000–
7 2009). *Journal of Geophysical Research: Earth Surface (2003–2012)*, 116(F2), 2011.
8 DOI: 10.1029/2010JF001757
9
- 10 Moon, T., Joughin, I.: Changes in ice front position on Greenland's outlet glaciers
11 from 1992 to 2007. *Journal of Geophysical Research: Earth Surface (2003–*
12 *2012)*, 113(F2), 2008. DOI: 10.1029/2007JF000927
13
- 14 Mortensen, J., Lennert, K., Bendtsen, J., Rysgaard, S.: Heat sources for glacial melt
15 in a sub-Arctic fjord (Godthåbsfjord) in contact with the Greenland Ice Sheet. *Journal*
16 *of Geophysical Research: Oceans (1978–2012)*, 116(C1), 2011. DOI:
17 10.1029/2010JC006528
18
- 19 Mortensen, J., Bendtsen, J., Motyka, R. J., Lennert, K., Truffer, M., Fahnestock, M.,
20 & Rysgaard, S.: On the seasonal freshwater stratification in the proximity of fast-
21 flowing tidewater outlet glaciers in a sub-Arctic sill fjord. *Journal of Geophysical*
22 *Research: Oceans*, 118(3), 1382-1395, 2013. DOI: 10.1002/jgrc.20134
23
- 24 Murray, T., Scharrer, K., James, T. D., Dye, S. R., Hanna, E., Booth, A. D. and 5
25 others: Ocean regulation hypothesis for glacier dynamics in southeast Greenland
26 and implications for ice sheet mass changes. *Journal of Geophysical Research:*
27 *Earth Surface (2003–2012)*, 115(F3), 2010. DOI: 10.1029/2009JF001522
28
- 29 Nansen, F.: *The first crossing of Greenland* Longmans, London, 1890.
30
- 31 Nick, F. M., Van der Veen, C. J., Vieli, A., & Benn, D. I.: A physically based calving
32 model applied to marine outlet glaciers and implications for the glacier

- 1 dynamics. *Journal of Glaciology*, 56(199), 781-794, 2010. DOI:
2 10.3189/002214310794457344
3
- 4 Nick, F. M., Luckman, A., Vieli, A., Van der Veen, C. J., Van As, D., Van de Wal, R.
5 S. W., Pattyn, F., Hubbard, A.L., Floricioiu, D.: The response of Petermann Glacier,
6 Greenland, to large calving events, and its future stability in the context of
7 atmospheric and oceanic warming. *Journal of Glaciology*, 58(208), 229-239, 2012.
8 DOI: 10.3189/2012JoG11J242
9
- 10 Pattyn, F., Schoof, C., Perichon, L., Hindmarsh, R. C. A., Bueler, E., de Fleurian, B.,
11 Durand, G., Gagliardini, O., Gladstone, R., Goldberg, D., Gudmundsson, G. H.,
12 Huybrechts, P., Lee, V., Nick, F. M., Payne, A. J., Pollard, D., Rybak, O., Saito, F.,
13 Vieli, A.: Results of the Marine Ice Sheet Model Intercomparison Project, MISMIP,
14 *The Cryosphere*, 6, 573-588, 2012. DOI:10.5194/tc-6-573-2012
15
- 16 Poulsen, J.: *Godthåb kommune*. KBK Netpublikation RI000059., Copenhagen, 1860.
17
- 18 Nick, F. M., Vieli, A., Andersen, M. L., Joughin, I., Payne, A., Edwards, T. L., Pattyn,
19 F., van de Wal, R. S.: Future sea-level rise from Greenland's main outlet glaciers in
20 a warming climate. *Nature*, 497(7448), 235-238, 2013. DOI: 10.1038/nature12068
21
- 22 Rayner, N. A., Parker, D. E., Horton, E. B., Folland, C. K., Alexander, L. V., Rowell,
23 D. P., Kent, E.C., Kaplan, A.: Global analyses of sea surface temperature, sea ice,
24 and night marine air temperature since the late nineteenth century. *Journal of*
25 *Geophysical Research: Atmospheres* (1984–2012), 108(D14), 2003. DOI:
26 10.1029/2002JD002670
27
- 28 Rignot, E., Fenty, I., Menemenlis, D., Xu, Y.: Spreading of warm ocean waters
29 around Greenland as a possible cause for glacier acceleration. *Annals of*
30 *Glaciology*, 53(60), 257-266, 2012. DOI: 10.3189/2012AoG60A136
31
- 32 Roussel, A.: Farms and Churches of the Medieval Norse Settlement in Greenland.
33 *Medelelser om Grønland*, 89(1), 1941.
34

- 1 Sciascia, R., Straneo, F., Cenedese, C., Heimbach, P.: Seasonal variability of
2 submarine melt rate and circulation in an East Greenland fjord. *Journal of*
3 *Geophysical Research: Oceans*, 118(5), 2492-2506, 2013. DOI: 10.1002/jgrc.20142
4
- 5 Sole, A. J., Mair, D. W. F., Nienow, P. W., Bartholomew, I. D., King, M. A., Burke, M.
6 J., Joughin, I.: Seasonal speedup of a Greenland marine-terminating outlet glacier
7 forced by surface melt-induced changes in subglacial hydrology. *Journal of*
8 *Geophysical Research: Earth Surface (2003–2012)*, 116(F3), 2011. DOI:
9 10.1029/2010JF001948
10
- 11 Straneo, F., Heimbach, P.: North Atlantic warming and the retreat of Greenland's
12 outlet glaciers. *Nature*, 504(7478), 36-43, 2013. DOI: 10.1038/nature12854
13
- 14 Straneo, F., Hamilton, G. S., Sutherland, D. A., Stearns, L. A., Davidson, F.,
15 Hammill, M. O., Stenson, G.B., Rosing-Asvid, A.: Rapid circulation of warm
16 subtropical waters in a major glacial fjord in East Greenland. *Nature*
17 *Geoscience*, 3(3), 182-186, 2010. DOI: 10.1038/ngeo764
18
- 19 Straneo, F., Sutherland, D. A., Holland, D., Gladish, C., Hamilton, G. S., Johnson, H.
20 L., Rignot, E., Xu, Y., Koppes, M.: Characteristics of ocean waters reaching
21 Greenland's glaciers. *Annals of Glaciology*, 53(60), 202-210, 2012. DOI:
22 10.3189/2012AoG60A059
23
- 24 Taurisano, A., Bøggild, C. E., Karlsen, H. G.: A century of climate variability and
25 climate gradients from coast to ice sheet in West Greenland. *Geografiska Annaler:*
26 *Series A, Physical Geography*, 86(2), 217-224, 2004. DOI: 10.1111/j.0435-
27 3676.2004.00226.x
28
- 29 Van Angelen, J. H., van den Broeke, M. R., Wouters, B., Lenaerts, J. T. M.:
30 Contemporary (1960–2012) evolution of the climate and surface mass balance of the
31 Greenland ice sheet, *Surveys of Geophysics*, 2013. doi: 10.1007/s10712-013-9261-
32 z.
33

- 1 Van As, D., M.L. Andresen, D. Petersen, X. Fettweis, J.H. van Angelen, J.T.M.
2 Lenearts, M.R van den Broeke, J.M. Lea, N. Bayou, C.E. Bøggild, A.P. Ahlstrøm, K.
3 Steffen.: Increasing meltwater discharge from the Nuuk region of the Greenland ice
4 sheet and implications for mass balance (1960-2012). *Journal of Glaciology* 220(60),
5 2014.
6
- 7 Van den Broeke, M., Bamber, J., Ettema, J., Rignot, E., Schrama, E., van de Berg,
8 W. J., van Meijgaard, E., Velicogna, I., Wouters, B.: Partitioning recent Greenland
9 mass loss. *Science*, 326(5955), 984-986, 2009. DOI: 10.1126/science.1178176
10
- 11 Vieli, A., Nick, F. M.: Understanding and modelling rapid dynamic changes of
12 tidewater outlet glaciers: issues and implications. *Surveys in Geophysics*, 32(4-5),
13 437-458, 2011. DOI: 10.1007/s10712-011-9132-4
14
- 15 Vinther, B. M., Andersen, K. K., Jones, P. D., Briffa, K. R., Cappelen, J.: Extending
16 Greenland temperature records into the late eighteenth century. *Journal of*
17 *Geophysical Research: Atmospheres* (1984–2012), 111(D11), 2006. DOI:
18 10.1029/2005JD006810
19
- 20 Weidick, A., Citterio, M.: The ice-dammed lake Isvand, West Greenland, has lost its
21 water. *Journal of Glaciology*, 57(201), 186-188, 2011. DOI:
22 10.3189/002214311795306600
23
- 24 Weidick, A., Bennike, O., Citterio, M., Nørgaard-Pedersen, N.: *Neoglacial and*
25 *historical glacier changes around Kangarsuneq fjord in southern West Greenland.*
26 Geological Survey of Denmark and Greenland. Copenhagen, 2012. ISBN: 978-87-
27 7871-347-6
28
- 29 Xu, Y., Rignot, E., Menemenlis, D., Koppes, M.: Numerical experiments on
30 subaqueous melting of Greenland tidewater glaciers in response to ocean warming
31 and enhanced subglacial discharge. *Annals of Glaciology*, 53(60), 229-234, 2012.
32 DOI: 10.3189/2012AoG60A139
33
34

1

2

1 Table 1. List of terminus observations and acquisition dates.

<i>Acquisition</i>		
<i>date</i>	<i>Observation type</i>	<i>Source</i>
1850s	Terrestrial photo'	H. Rink (in Weidick et al, 2012)
1859	Map	Kleinschmidt (1859)
1860	Map	Poulsen (1860)
1866	Map	Rink (1866)
1866	Map	Falbe (1866)
1885	Map	Jensen (1885)
1880s?	Sketch (after photo')	Nansen (1890)
1903	Terrestrial photo'	J. Møller in Bruun (1917)
1921	Terrestrial photo'	A. Nissen in Weidick et al (2012)
1932	Terrestrial photo'	A. Roussell in Roussell (1941)
27/08/1936	Oblique photo'	Weidick et al (2012)
10/08/1946	Oblique photo'	Weidick et al (2012)
20/08/1948	Oblique photo'	Weidick et al (2012)
21/06/1965	Terrestrial photo'	Weidick et al (2012)
16/08/1968	Aerial photo'	USGS
15/09/1979	Terrestrial photo'	Weidick et al (2012)
15/09/1987	Satellite	Landsat
19/09/1992	Satellite	Landsat
30/08/1993	Satellite	Landsat
18/09/1994	Satellite	Landsat
14/10/1995	Satellite	Landsat
14/09/1996	Satellite	Landsat
01/09/1997	Satellite	Landsat
15/09/1999	Satellite	Landsat
18/09/2000	Satellite	Landsat
22/10/2001	Satellite	Landsat
23/09/2002	Satellite	Landsat
09/08/2003	Satellite	Landsat

12/09/2004	Satellite	Landsat
24/09/2005	Satellite	Landsat
18/09/2006	Satellite	Landsat
27/09/2007	Satellite	Landsat
23/09/2008	Satellite	Landsat
19/09/2009	Satellite	Landsat
13/09/2010	Satellite	Landsat
16/09/2011	Satellite	Landsat
18/09/2012	Satellite	Landsat

1

2

3

1 Table 2. List of parameters and constants used for running the model

<i>Parameter/Constant</i>	<i>Value</i>
Ice density – ρ_i	900 kg m ⁻³
Meltwater density – ρ_w	1000 kg m ⁻³
Proglacial water body density – ρ_p	1028 kg m ⁻³
Gravitational acceleration - g	9.8 m s ⁻²
Friction exponent - m	3
Friction parameters – μ and λ	1
Glen's flow law exponent - n	3
Glen's flow law coefficient - A	4.5 x 10 ⁻¹⁷ Pa ⁻³ a ⁻¹ (-5°C)
Grid size	~250 m
Time step	0.005 a

2

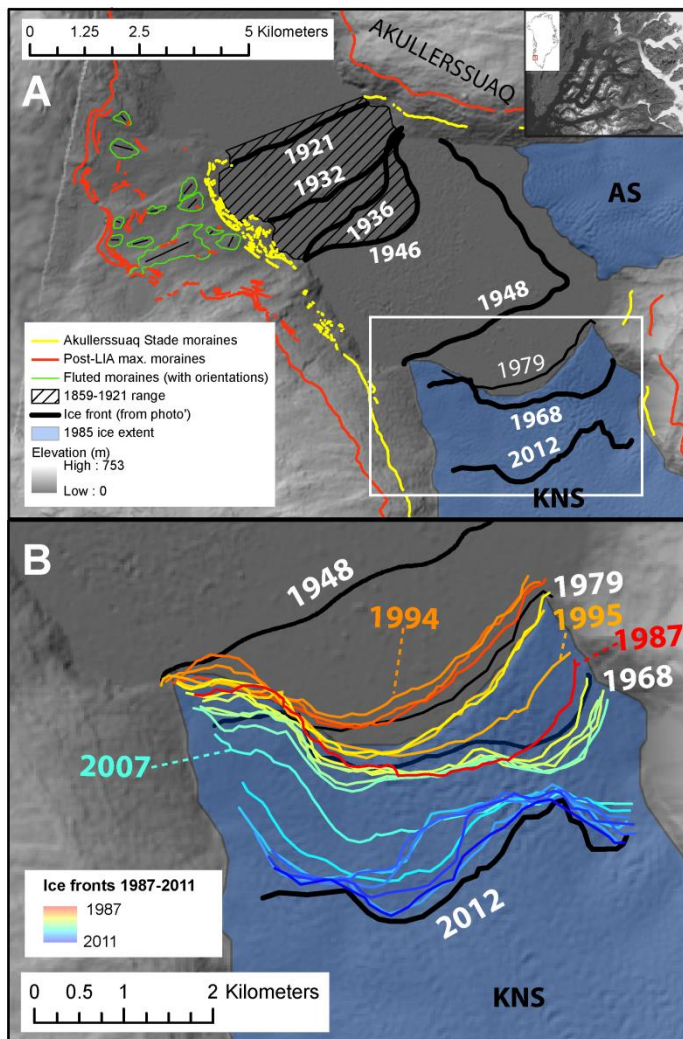
3

4

1 Table 3. Pearson correlation coefficient values for tuning parameters of successful
 2 model runs (n = 29). Correlation coefficients with p-values <0.05 are highlighted in
 3 bold.

	α_1	α_2	α_3	<i>Mbase</i>
α_1	-	-0.92285	0.287883	-0.46884
α_2	-0.92285	-	-0.46065	0.292157
α_3	0.287883	-0.46065	-	-0.42711
<i>Mbase</i>	-0.46884	0.292157	-0.42711	-

4
 5
 6
 7

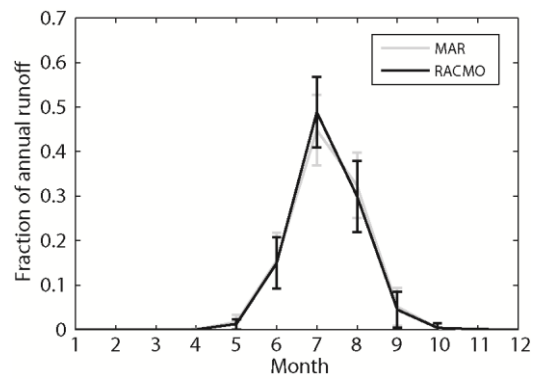


1

2 Figure 1. Diagrams showing the site location (inset), terminus positions and
 3 geomorphology plotted on a hillshaded mosaic of a stereophotogrammetrically
 4 derived digital elevation model (DEM) from images acquired in 1985, and ASTER
 5 GDEM (Hvidegaard et al., 2012). (A) termini and geomorphology for 1859-2012, with
 6 ASM limits delineated in yellow, and (B) a detailed view of termini for the period
 7 1948-2012, with specific years labelled for reference.

8

9



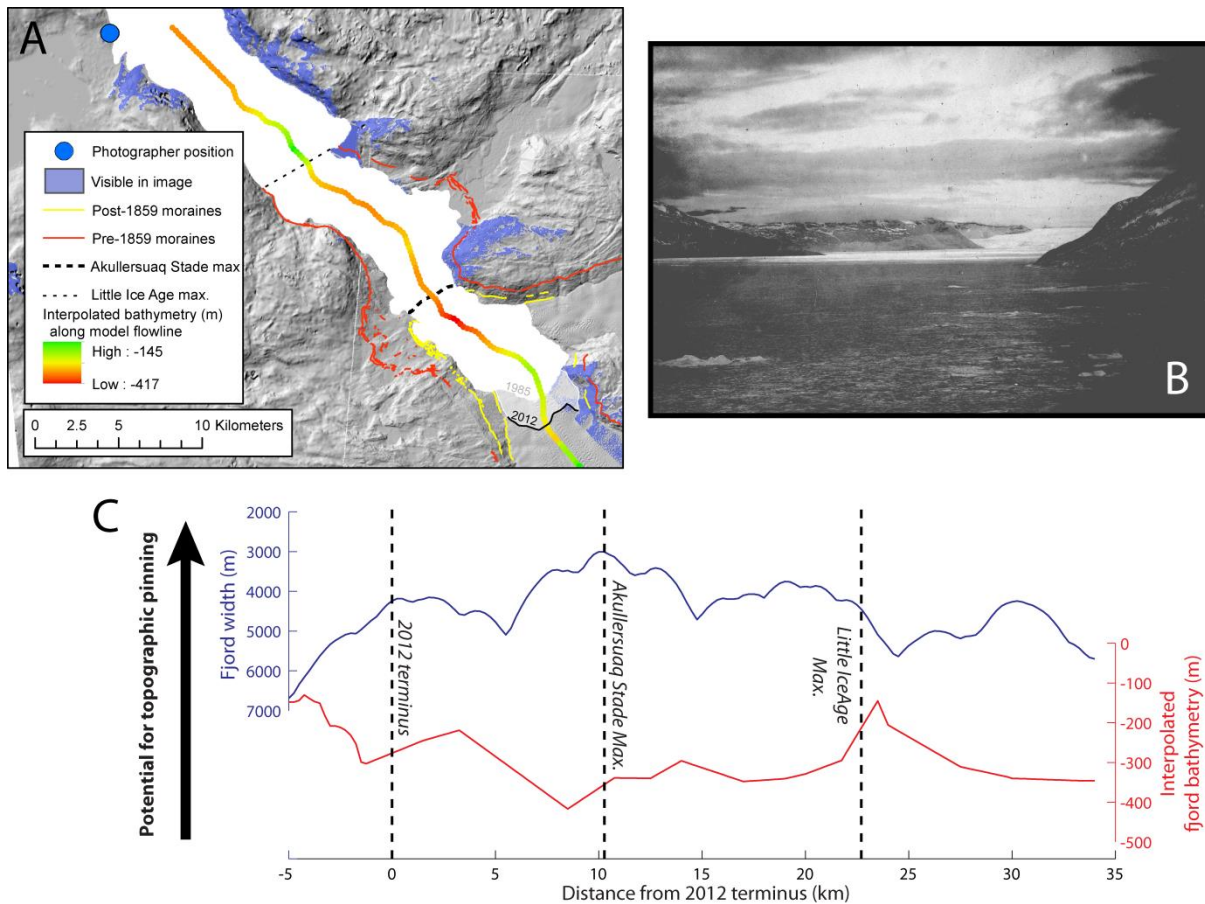
1

2 Figure 2. Fraction of annual runoff occurring for each month as given by MAR and
3 RACMO2 SMB models for KNS and AS between 1960-2012 (Van As et al., in
4 press). Error bars are given to 2 standard deviations.

5

6

7



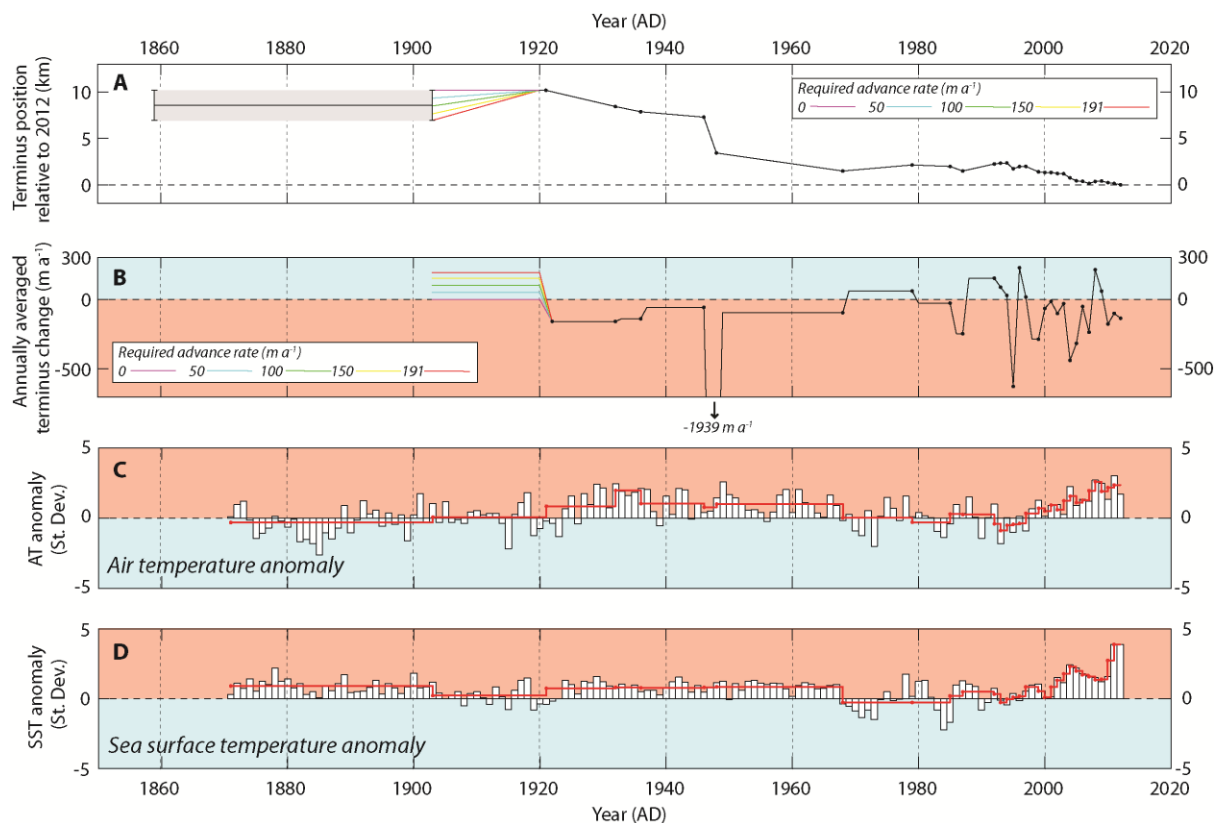
1

2 Figure 3. Viewshed analysis. (A) 1985 hillshaded DEM (see Figure 1), with
 3 reconstructed photographer position showing areas that would be observable in the
 4 photograph, and the path of the model flowline showing the interpolated fjord
 5 bathymetry, (B) the photograph of KNS acquired in 1903, (C) along-fjord width and
 6 depth relative to the 2012 terminus position. Note that fjord width is plotted on a
 7 reversed axis to reflect the relative potential for the occurrence of topographic
 8 pinning points.

9

10

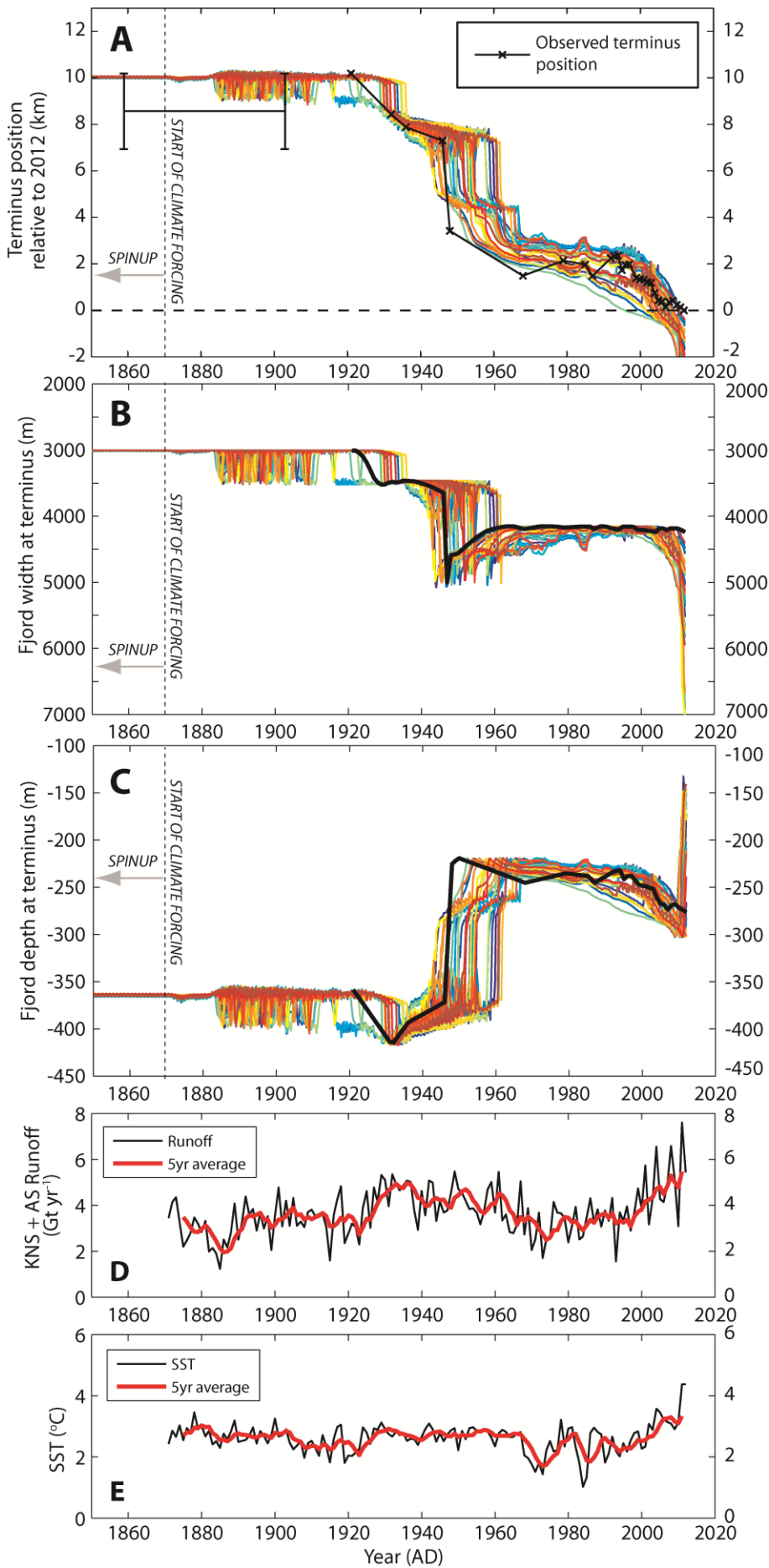
11



1

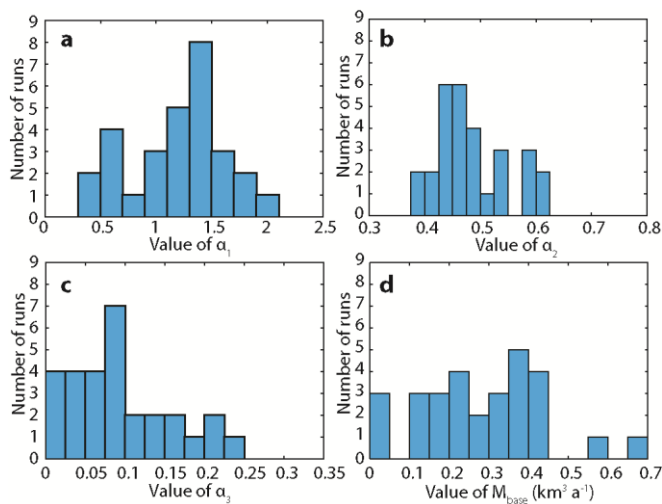
2 Figure 4. (A) Terminology change relative to the 2012 terminus position. Uncertainty in
 3 terminus position for 1859-1903 highlighted in grey, with a range of potential
 4 advance rates for 1903-1920 indicated. These range from a minimum of no change
 5 (0 m a^{-1}) to a maximum possible advance rate of 191 m a^{-1} . (B) Annually averaged
 6 rates of terminus change between observations (black dots). Includes terminus
 7 advance rates described for 1903-1921 terminus change indicated on A. (C)
 8 Summer ATA (June, July, August) at annual resolution (white bars), and red line
 9 showing the averaged ATA between terminus observations (Cappelen et al, 2012;
 10 Vinther et al, 2006). (D) Annual SSTA for the area 61° to 65° N 51° to 56° W at
 11 annual resolution (white bars) and red line showing the averaged SSTA between
 12 terminus observations (Rayner et al, 2003).

13



1 Figure 5. (A) Evolution of terminus position for model runs (coloured lines)
 2 determined to be successful according to the criteria outlined in the text, with
 3 observed terminus position also plotted (bold black line, with positions between
 4 observations linearly interpolated). (B) Evolution of fjord width at the terminus, with
 5 values interpolated from observations plotted in black, (C) Evolution of fjord depth at
 6 the terminus, with values interpolated from observations plotted in black, (D)
 7 Combined KNS and AS runoff volume estimates for 1871-2012 that are used to
 8 drive the model (5 year moving average also plotted in red). (E) Absolute annual
 9 SST estimates used to drive the model from Rayner et al. (2003) for the area 61° to
 10 65° N and 51° to 56° W (5 year moving average also plotted in red).

11



12

13 Figure 6. The distribution of the tuning parameters (a) α_1 (bin width = 0.2), (b) α_2 (bin
 14 width = 0.025), (c) α_3 (bin width = 0.025), and (d) M_{base} (bin width = 0.05 $\text{km}^3 \text{a}^{-1}$) for
 15 successful runs as defined by the criteria outlined in the text. Minimum and
 16 maximum x-axis values represent the full range of values tested within the 1500
 17 model runs.